



OTC 19525

## Virtual Metering Technology Field Experience Examples

Prashant Haldipur, Ph.D., SPE; Gregory Metcalf, SPE; Multiphase Solutions, Inc.

Copyright 2008, Offshore Technology Conference

This paper was prepared for presentation at the 2008 Offshore Technology Conference held in Houston, Texas, U.S.A., 5–8 May 2008.

This paper was selected for presentation by an OTC program committee following review of information contained in an abstract submitted by the author(s). Contents of the paper have not been reviewed by the Offshore Technology Conference and are subject to correction by the author(s). The material does not necessarily reflect any position of the Offshore Technology Conference, its officers, or members. Electronic reproduction, distribution, or storage of any part of this paper without the written consent of the Offshore Technology Conference is prohibited. Permission to reproduce in print is restricted to an abstract of not more than 300 words; illustrations may not be copied. The abstract must contain conspicuous acknowledgment of OTC copyright.

### Abstract

This paper discusses the recent advances made in virtual well metering technology and presents the experience gathered from deploying the technology in the Gulf of Mexico and various other locations globally over the last five years. Project execution best practices, including specifications, acceptance testing and commissioning procedures, are presented for deploying this advanced technology.

The paper presents field data comparison and shows that this technology has provided very reliable and accurate flow rate predictions over a variety of well configurations and reservoir characteristics (from gas condensate to black oil systems over a wide range of GOR/GLRs). The value of the dynamically estimated flowrate uncertainties in addition to real-time, continuous well flowrate estimates is described. These systems are equipped with real-time calibration programs that reconcile the total well production, on a daily or weekly basis, with the fiscal production and then back-allocate the production to the wells based on the calculated well flowrate uncertainties.

These well metering systems are easily integrated with real-time pipeline flow monitoring systems to provide real-time advisory capability to the operator. These systems have expanded in recent years to include leak detection/restriction detection capabilities, look-ahead/forecasting capabilities that offer flow assurance guidance on operational issues such as cool-down, warm-up and hot-oil circulation times, and the paper presents such examples.

### Introduction

Multiphase flow simulation technology has matured to the point where it is frequently used to tackle flow assurance problems during design as well as day-to-day operation of oil and gas pipelines. Simulations are used, for example, in sizing pipes and thermal insulation; developing procedures for start-up, shutdown, and process upsets; and avoidance of wax and hydrate formation. An emerging application area is “online” simulators [Parthasarathy, P. et al., 2007] which are integrated with field data acquisition systems (DCS/SCADA). The demands on online systems differ considerably from design simulation tools [Llave S., 2005]. Design tools can assume idealized conditions, with precise knowledge of process parameters (inlet/outlet pressures and flowrates, fluid compositions, etc.). Corresponding measurements are often unavailable in the field. Numerical models must therefore be flexible to use such data as available. Models must handle instrument drop-out, noise, bias and drift, and incorporate filtering to stabilize the numerical model. Compositional uncertainties must be addressed by building in tuning factors so that predictions match the measured outlet phase rates. Online simulators are key to implementing model-based leak/restriction detection systems, which are the only viable systems for subsea multiphase pipeline networks [Scott, S.L and Barrufet, M.A., 2003].

Real-time readings from the gas and liquid export flow meters are usually available for export pipelines that extend from the offshore platforms to shore receiving facilities. These rates are used to feed online simulators via the field data acquisition systems (DCS/SCADA). These online simulators in turn provide real time information on pipeline holdup, pressure, flowrate, and temperature profiles; arrival slug size; pig tracking; and proximity to hydrate or wax formation. A powerful application is to combine field data and online model predictions to run look-ahead simulations. For example, safe pigging campaigns can be planned to ensure that the swept liquids will not flood the slug-catchers [Haldipur, P. et al., 2007].

For simulating infield subsea flowlines that extend from the wells to topsides, a common problem is the lack of real-time three-phase flowrates from the wells. One option is to install subsea physical multiphase flowmeters, but this is expensive; also, testing, calibration, and post-installation tuning of these meters are often problematic. Further, for subsea installations, it is not economically viable to remove these meters in order to carry out any type of maintenance if needed. Increasingly, operating companies are turning to software based solutions to estimate the well flowrates in real time.

This technology is known as virtual metering. Virtual Metering Systems (VMS) use the existing pressure and temperature measurements in and around the well to estimate the well flowrate. Multiphase Solutions (MSi) first deployed VMS in the

late 1990's in the Southern North Sea, and the technology has since matured into a robust product that is able to overcome all the real-life installation issues such as data unavailability, system maintainability, etc., and provide fairly accurate results [Picart, P. and Llave, S. 2004].

This paper is organized as follows. First, we present an outline of VMS technology. Next, we discuss field performance of stand-alone VMS for gas-condensate and black-oil systems. Finally, we present some examples where VMS have been used for flow assurance applications including leak and restriction detection.

### **Description of Virtual Metering Systems**

VMS estimates the three-phase well flowrates in real time using existing instrumentation within the wellbore and on the wellhead and Christmas tree. The software is based on models that extend from the reservoir to downstream of the wellhead choke. Usually, there is adequate information/instrumentation available to use multiple independent models to estimate the well flowrate. Multiple estimates make predictions more accurate and the technique robust and tolerant to instrumentation failures. Typical measurements used by the system are:

- Bottom-hole pressure and temperature
- Before choke pressure and temperature
- After choke pressure and temperature
- Choke position
- Master, Wing, and Shutdown valve status

### **Modeling**

The models used to construct these systems are discussed here. The four building blocks that make up the system are: (i) a near-wellbore reservoir model, (ii) a transient wellbore model, (iii) a choke model, and (iv) a well jumper model. The near-wellbore reservoir model is used to provide the pressure boundary which in conjunction with the well inflow performance characteristics (IPR/PI) is used to estimate the flowrate across the perforations. In some cases, the near-wellbore reservoir model is substituted by a constant reservoir pressure boundary condition; in other cases, where the cumulative depletion from the reservoir can be calculated by VMS in real time, a pressure vs. cumulative-production depletion curve is used. The full-stream fluid composition, wellbore profile (vertical depth vs. measured depth), tubing diameter(s) and roughness(es), and the geothermal gradient are used to configure the wellbore model, which predicts transient three-phase flow in the well. The mass-conservation equation, the momentum-balance combined with appropriate closure laws depending on the flow regime, and energy-balance equations, are solved for the flowrate in the wellbore using all available pressure and temperature data. The choke model uses the choke  $C_v$  relationship with pressure and temperature measurements across the choke to estimate the flowrate.

### **Methods**

The key to accurate flow rate estimation is the use of multiple methods/techniques. Some approaches are more accurate than others in specific flow regimes. VMS uses several methods to estimate the flowrate. These methods are different combinations of the basic building blocks, discussed above, and employ a subset of the real time measurements for their boundary condition. The various methods are enumerated below.

- Method #1 extends from near-wellbore reservoir to manifold (at end of well jumper)
- Method #2 extends from near-wellbore reservoir to downstream of choke
- Method #3 extends from near-wellbore reservoir to upstream of choke
- Method #4 extends from bottom-hole to manifold (at end of well jumper)
- Method #5 extends from bottom-hole to downstream of choke
- Method #6 extends from bottom-hole to upstream of choke
- Method #7 extends from near-wellbore reservoir to bottom-hole
- Method #8 extends across choke
- Method #9 extends across the well jumper

Figure 1 shows the effect of using these methods at various choke positions. The analysis is based on a VMS that was recently deployed for subsea wells in a gas-condensate reservoir in the Asia-Pacific region. Each of the nine methods used provides a flowrate estimate and an associated uncertainty estimate. The uncertainty estimate is obtained by perturbing the measured pressures, temperatures, and choke position, and calculating the deviation in the flowrate estimate. Pressures and temperatures are perturbed by the transmitter accuracy provided by the manufacturer. The choke position is perturbed based on a user-provided uncertainty. The error in estimating the position of subsea chokes is dependent on the method used for determining the position – whether the system is using the inferred value from choke steps and what the operational history suggests (e.g. whether the system was re-calibrated when not at true zero), or whether the system uses LVDT measurement. VMS combines the flowrates obtained from the individual methods and provides a best estimated flowrate and an overall uncertainty for the prediction.

As shown in Figure 1, the overall uncertainty is non-monotonic and peaks at a choke opening of 20%. The high uncertainty at low choke openings can be attributed primarily to the choke method (method #8) and to a lesser degree to methods #3 and #6. Conventional wisdom is that the choke model is very accurate at low choke positions and becomes increasingly inaccurate as higher choke openings. This is true as far as absolute values are concerned, but not quite true in

terms of percentage errors. At low choke openings, the choke method (method #8) is sensitive to errors in measured choke position, while at higher openings, it is most sensitive to measurement errors in the upstream and/or downstream pressure.

For the case shown in Figure 1, the Cv for this choke is pretty flat below 20% and then starts increasing rapidly such that the percentage change in Cv (i.e.,  $\Delta C_v/C_v$ ) is highest near an opening of 20%. Thus, a bias error in the choke position measurement would yield the largest percentage error when the choke is 20% open. At choke opening beyond 60%, the pressure drop across the choke is small and errors in the before/after choke pressure measurement result in a substantial variation in the estimated flowrate causing the uncertainty to be high at large openings.

The methods not integrated with the choke – methods 3 and 6 – provide a much higher flowrate estimate and very high uncertainty at low choke positions, i.e. at low flowrates. At low flowrates, there is hardly any frictional drop in the well and flowrate estimate is very sensitive to the estimated static head in the well. Any inaccuracies in the fluid composition would result in errors in the estimated static head, due to errors in estimating gas and/or liquid densities, and will cause a large error in the estimated flowrate. These methods work better at higher flowrates when the frictional drop is a significant portion of the total pressure drop in the well. The IPR/PI method (method #7) also has a high uncertainty at low flowrates when the pressure drop across the perforations is small. The well jumper method also exhibits a similar behavior.

The key is to combine these various methods to obtain a robust estimate with the lowest overall uncertainty.

### Robustness

Experience has taught us that one cannot build a system that relies on all subsea instrumentation to be working throughout field life. Downhole gauges are known to fail within a few years of installation, sometimes even within the first year. Even wellhead instrumentation will fail, though there is enough redundancy in these to safely expect to receive the wellhead pressure and temperature data throughout field life. Figure 2 shows the performance of the same system (as in Figure 1) when all instruments except one pressure-before-choke transmitter, one temperature-before-choke transmitter, and the choke position sensor, fail. Method #3 that uses the reservoir pressure and before-choke-pressure measurement is used to estimate bottom-hole pressure and temperature to feed methods #6 and #7. The other methods (#1, #2, #4, and #5) that use a wellbore model integrated with the choke model automatically truncate the model at the choke, thereby becoming identical to methods #3 and #6, but report a high (default) uncertainty value because of the failed instrument downstream of the choke. The choke model reports the critical flowrate through the choke along with a high (default) uncertainty. When all the methods are combined, the best estimated flowrate is quite close to the actual value, as shown in Figure 2.

### Well Surveillance

Figure 3 shows a typical screen from a VMS application that details all the key information regarding the well. At the bottom of the screen, the estimated gas and liquid flowrates from each of the methods are listed along with the calculated uncertainties. The screen also lets the user turn-off specific models via a check-box – in the displayed figure, method #9 has been turned off. The system uses real time calibration programs that reconcile the total well production, on a daily or weekly basis, with the fiscal production and then allocate the production back to the wells based on these calculated well flowrate uncertainties. The screen also contains a graphical display of the estimated flowrates from each of the methods with their individual uncertainties (plotted as error-bars). The best estimated flowrate is shown by a red line and the overall uncertainty is depicted by a grey band across the red line.

On top of the screen, the user can choose different flash conditions – after-choke condition, before-choke condition, separator condition, or reservoir condition – to display the mass and volume rates. The well flow summary table automatically updates to report the well rates at that flash condition.

The screen also summarizes the key instrument readings for the well including valve status/positions. The system has well surveillance intelligence built-in. In the displayed figure, each of the methods show a large temperature (dT) error between the model estimated before/after-choke temperatures and the measured temperatures. Since the error is consistent across all the methods, the most likely explanation is that the instrument reading is defective. Consequently, the system automatically does the following:

- Highlights (red) the before- and after-choke temperature measurement displays
- Raises the reliable data alarm
- Raises the overall health alarm

These visuals help the operator in quickly locating the source of the error (in this case, the temperature transmitters) and enables prompt intervention.

### Field Examples of Standalone Applications

The primary purpose of standalone virtual metering applications is providing real time well flowrate estimates and to help reconcile daily/monthly production back to the wells. They may also serve secondary purposes such as optimizing methanol injection rates and providing information for sand monitoring.

#### Gas-condensate field examples

We recently commissioned a VMS for a four well subsea development in the Asia Pacific region in roughly 130m water depth. The wells are tied-back to the platform via a 24 km pipeline. Three of the wells are from one reservoir producing lean gas/condensate with CGR in the range of 30-50 bbl/MMscf. The nominal production from these wells is in the range of 250-350 MMscfd. The fourth well is from another reservoir producing rich gas/condensate with CGR in the range of 150-200 bbl/MMscf. Formation water cut is less than 2% during early life.

All wellheads are instrumented with dual pressure and dual temperature sensors. In addition, subsea differential pressure sensors are used to accurately measure the dP across the choke. A cableless downhole PT gauge is installed close to the perforations – the battery life of the gauge is expected to be approximately two years and during this period, the VMS was designed to use the cableless gauge readings. A wired downhole PT gauge is installed mid-way through the wellbore and the system is designed to switch over and use the wired gauge after the cableless gauge stops working.

#### ***Secondary functions***

A venturi meter is also installed at the top of the riser to measure the commingled production from the four (4) subsea wells. VMS is used to predict the commingled gas density, liquid density, and the isentropic exponent ( $k \equiv C_p/C_v$ ), at the venturi PT conditions. These values are used by the venturi meter software for its calculations. VMS is also used to predict the total volumetric flowrate at the wellhead condition and this information is relayed to the sand detection equipment software and used for monitoring sand production.

An important function that VMS performs in this installation is to predict the well flowrates during bean-up. During shut-in periods, the flowline is depressurized to mitigate the risk of forming hydrates. During startup, the riser boarding valves are kept shut and the flowline is slowly pressurized up by opening one or more of these wells. During this bean-up period, the operators are completely reliant on the well flowrates predicted by VMS. They use these predicted rates and the observed rate of change in the pipeline pressures to infer whether they have a hydrate blockage within the flowline.

#### ***Factory Acceptance Testing***

The system was configured to obtain data from the ABB Infi90 PCS via an ABB Harmony OPC server. A crucial decision taken during project execution was to perform the FAT with a test server connected to the PCS hardware (PCS rack) and loaded with the actual tag names. As a result, we were able to load our system with the correct tag names and iron out several connection issues ahead of time without having to deal with these offshore during commissioning and startup. One issue was that VMS was designed as per client's functional specification to use two separate digital tags per valve, e.g. "verified open" = 1 and "verified close" = 0 to indicate that the valve is open. During FAT, we discovered that the as-built OPC server used a single tag (0-100%) for each valve and were able to rectify the software in the factory before shipment. Another issue that arose during the FAT was how to verify that the communication between the VMS OPC client and ABB OPC server was working. In the end we ended up modifying the system to add a heartbeat signal on the OPC client side and logic on the OPC server side to interpret the heartbeat signal. Other issues that were discovered and resolved were to deal with how the two systems communicated with respect to (i) a wrong or missing tag within a group validation request, (ii) interpreting the bad data quality bit in a tag, (iii) mapping of tri-state alarms (good/marginal/bad) on the OPC client side to a dual state alarm (good/bad) on the OPC server, and (iv) presence of tags that have an "empty" value but a good data quality bit – a situation that happens on an equipment power cycle. As a result of taking these steps, there were no communication issues encountered during the system commissioning offshore – an extremely rare occurrence. Typically, considerable portion of time during commissioning is spent addressing system integration problems, leaving little time for system tuning and model verification.

#### ***Commissioning Plan***

This system was installed offshore before the wells started flowing. The plan was to bring the wells on one-by-one and flow them into a dedicated production separator topsides for an extended window of time. This production plan allowed accurate field calibration/tuning of VMS. The first well would be tuned based on the gas and liquid flowmeters on the production separator trains and after the first well is calibrated, subsequent wells would then be brought on and tuned by difference. The first well would carefully be ramped up to allow calibration at a number of choke positions. Since VMS does not incorporate the 24 km subsea tieback and hence cannot replicate its flow dynamics, the choke was held steady for six hours at each position during commissioning to allow the flowline to reach steady state, thereby allowing the tuning to be done when the system is at steady state.

#### ***Well Testing***

During the initial production clean-up process, the first well to be started-up was tested using a mobile well-testing rig. We were informed by the client that the well fluid was relatively clean during the well-test and, in preparation of VMS commissioning, we should tune to the well-test CGR. As it transpired, the well was not completely clean at the time it was tested and the well test data provided a higher CGR. Consequently, VMS predicted a lower gas mass fraction during commissioning; Figure 4 shows the system predictions of gas mass fraction during commissioning and after tuning the system. Note that the gas mass fraction data during the initial part of commissioning phase should be discarded. At the lowest choke position, the liquid flowrate was lower than the turn-down of the turbine meter and hence recorded as zero. Hence, the measurements suggest erroneously a GMF equal to 1 at the lowest choke position.

#### ***Commissioning***

Just prior to commissioning, we had to make a few major adjustments. The cableless gauge was updating only once in four days to conserve battery life and therefore, the bottom-hole methods had to be temporarily disabled. The differential pressure sensor readings were capped at a low value – the choke method had to be modified not to use these readings. Figure 5, Figure 6, and Figure 7 compare the performance of the untuned (out-of-the-box) system during commissioning. The total mass rate predictions were only slightly lower and within 10% of the measured value. Since the GMF was tuned to a lower value of 0.8 (based on the well-test), the errors in the gas mass rate predictions appear amplified. Note that the VMS rates are the wellhead rates flashed dynamically at the separator pressure and temperature conditions and do not incorporate the

dynamics of the 24 km flowline. Moreover, the separator liquid outflow is controlled by a level controller. In addition, a well rampup will result in a liquid surge from the flowline while a rampdown will cause a decrease in the liquid outlet due to corresponding increase in the pipeline holdup. To account for these fluctuations, the choke was held at each position for 6 hours in order to let the system reach steady state and enable VMS to be tuned to these conditions.

After commissioning, the system was tuned based on the latest available data. The key changes made were: (i) the near-wellbore reservoir pressure was updated based on the cableless gauge data, (ii) wellbore profile was updated based on as-built drawings, (iii) the wired downhole gauge locations were updated based on the as-built drawings and the bottom-hole methods were reconfigured to use the wired downhole gauge, (iv) the wellstream composition was updated based on PVT analysis collected during commissioning, (v) the choke Cv profile was adjusted, (vi) the tubing roughness and heat transfer coefficients were also modified, and (vii) the well IPR was modified based on the updated information provided by the reservoir engineers. These changes are not time consuming; the system was reconfigured in less than a week. Figure 5, Figure 6, and Figure 7 also depict the performance of the system after it has been tuned; it is clear that excellent agreement is achieved between predictions and measurement after tuning.

#### ***Tuning by Difference***

Once the first well has been tuned and the system offshore had been upgraded with the latest configuration patch, the commissioning and tuning of the second well was carried out. The same procedure was followed for the third and fourth wells. Figure 8 and Figure 9 show the predictions of VMS (after tuning) for both wells (well 1 & 2) flowing into the same production separator; again agreement between predictions and measurement is excellent. Other wells (both platform and subsea) were routed to another separator for the duration of the test period. Since the same choke was fitted on all the wells, only the first well was tested at multiple choke positions. Subsequent wells were tested at a single choke position to minimize the disruption to the platform production.

During the tuning process, we try to match the flowrates as well as the measured pressures and temperatures at the wellhead and within the wellbore. This ensures that the model has been correctly tuned. Figure 10 compares the model predicted pressure at the downhole gauge, located mid-way through the wellbore, to the measured pressure. A close match between the model predictions and measurement verifies that the distributions within the wellbore of the liquid holdup, the frictional resistance, and the fluid temperature, have been accurately captured by the model.

#### ***Historical Results***

Consider another VMS installation in the Asia Pacific region, but one that has been operational since 2001. This is a five well subsea installation in 800 m water-depth with a 30 km dual flowline tieback to a platform. The historical accuracy of this installation is shown in Figure 11. Over the last 2 years, the monthly reconciliation factors have been less than 5%, and roughly 2.5% on the average.

In Q2 of 2005, we saw that the reconciliation factors suddenly increased; these dates are marked in Figure 11. On investigation, we found that these were due to communication problems, resulting in VMS receiving erroneous readings. Figure 12 shows a sampling of the data problems that were encountered – the pressure before choke values were getting multiplied by a factor of 2 or 3 before getting to the system. Subsequently, we added some custom filtering techniques and logic to correct the data. The improved filtering techniques recognize inconsistent instrument readings and compensate where applicable. Using these techniques, we were able to reduce the reconciliation factors to 7.5% as shown by the red bars in Figure 11.

#### ***Methanol Injection***

In this five well subsea system, the virtual metering predictions are used to control methanol injection. The market value of the condensate can be severely affected by the level of methanol contamination. The predicted well flow rates are used to figure out the total methanol injection rate required and to proportion it to the individual wells. The desired operational goal is to keep the methanol concentration at 50%; see Figure 13 for a plot of the measured concentration. As can be seen from the figure, the system enables the operators to optimize their methanol injection fairly well.

#### **Black-oil field examples**

Here we present our experience in deploying this technology in the Gulf of Mexico. This development is in approximately 1300m water-depth. The wellbores are themselves quite deep (having approximately 5500m TVD) and the wells are tied-back to the platform via a dual-flowline piggable loop.

This development had concerns of: (i) asphaltene deposition, (ii) hydrate formation, and (iii) paraffin wax deposition. So we deployed not only VMS to allocate production back to the wells, but also integrated it with a real time pipeline flow simulator. The pipeline simulator would receive the real time flowrates from VMS and monitor the flows, pressures, temperatures, and compositions within the dual-flowline loop. The system would then provide the following monitoring information: (i) location where the fluid is crossing the bubble-point (likelihood of asphaltene deposition), (ii) approach to hydrate formation temperatures within the flowline, and (iii) approach to wax appearance temperatures within the flowline.

#### ***Lessons Learned***

- Communications testing should be performed with actual tags and with the field system that is going to be installed
- Communicate with the actual tag server wherever possible. Chances of data dropout increases as the number of data I/O layers increases between the actual tag server and your OPC client

- Try to get data from an OPC server that feeds data to the control room or to multiple applications – chances of problems being noticed early increases
- Remote access, especially for offshore installations, will greatly improve the response time and help vendors in monitoring the system performance closely
- Make the system as simple as possible.

#### ***Modular Approach vs. Integrated Approach***

During design, it was decided that VMS and the pipeline management system would be tightly coupled. If there is no flow path between the well and the topside separator, then the system would not predict the well flowrates since it would not know which flowline to push the flow into. At site, we found that the valve signals were simply not reliable. Figure 14 shows the flip-flopping signals received for the flow isolation valves (FIVs). At times, the data would show that both the FIVs were open; this was not possible due to a valve interlocking system that would not allow any well to be lined up to both flowlines simultaneously. At other times, the data would show that wells 1&2 were lined up to flowline A when, in reality, both the wells were lined up to flowline B.

To overcome this difficulty, we modified the software to add manual overrides for the well-to-flowline and flowline-to-separator alignments. We added a summary screen, shown in Figure 15, showing flow path alignments from wells to separators. We also added a detailed alignment screen, shown in Figure 16, which showed the status of all the valves used by the system. Green signifies that the valve is open; red signifies that the valve is closed; and yellow signifies that conflicting data has been received regarding the valve status. The screen also contained a panel for user override of the flow path alignment.

#### ***Using measured water cut***

During design, the customer preferred using the instantaneous water volume rate predictions from the topsides physical multiphase meter to infer the water cut and use it as an input for VMS. Figure 17 shows the oil volume rate, water volume rate, and the water cut information inferred from the multiphase meter during the early months following 1<sup>st</sup> oil. We found several issues with the water volume rate measurements: (i) they were often negative (capped to zero by the VMS OPC client) or zero; see the water volume rate before 1/6/2007; (ii) though the oil volume rates are continuously changing, the water volume rates show a step-like response. From 1/6/2007 to 1/8/2007, the production ramped up from 0 to 15 Kbpd but the water volume rates remained steady at 375 bpd. After 1/10/2007, though the oil volume rates showed a steady decline, the water volume rates remained steady (and in fact, jumped up on 1/15/2007). Consequently, the inferred water cut values fluctuated a lot as shown in Figure 17. All this led us to disable the automatic water-cut update feature and instead change it to a user-input for each well.

#### ***Performance***

After tuning, VMS compared very well with the production separator gas and liquid leg measurements. We were able to tune well 2 using a standard depletion curve for the reservoir pressure; see Figure 18 for a comparison between the VMS predicted flow rates and the measured flowrates. The gas rates are being slightly underpredicted but the oil rates are right on target.

For another well, i.e. well 1, we found that using a standard depletion curve model resulted in a significant overprediction; see the (untuned) well 1 result shown in Figure 19 (a) and (b) and compare that to the well 3 result shown in the same figure. Figure 19 (c) also shows that there is no pressure-drop across the choke for well 1 – making the choke method useless. The pressures within the wellbore (bottom-hole and before-choke) drop rapidly after well startup. This combined with a nearly-constant reservoir pressure boundary condition yields a very high flowrate prediction.

Note that the VMS results are predicted at the wellhead and dynamically flashed at the separator conditions and do not incorporate the dynamics of the dual flowline loop. Following well 3 startup, the oil rate at the separator reaches steady state within one day while the gas rate takes several days to reach steady state due to linepacking of the flowline; note that the GOR of well 3 is much higher than that of well 1 or well 2. Contrast the well 3 startup behavior to that of well 1. Both the separator oil and gas rates quickly reach a peak and then begin declining rapidly. The contrast between the well 1 and well 3 behaviors can also be observed in the pressures; see Figure 19 (c). Well 1 bottomhole and before-choke pressures rapidly decline following startup and build up slowly after shutdown, while well 3 bottomhole and before-choke pressures reach a steady value fairly quickly after startup and also build up rapidly after shutdown. The data does point out that the near-wellbore area of well 1 does not fill up rapidly enough to sustain the pressures.

We ended up adding a near-wellbore reservoir tank model that would model the near-wellbore pressure buildup during periods of well shut-in and the rapid depressurization that would ensue after the well started flowing. After incorporating this, we were able to match the field predictions for well 1 very well; see Figure 19 (a) and (b).

#### ***Flow Assurance Advisory***

Since these systems are integrated with a real time transient pipeline flow model, overpredicting or underpredicting the well flowrates has a direct consequence on the flow assurance advisories conveyed by the pipeline management system. Figure 20 shows that overpredicting the (untuned) well 1 flowrate based on a nearly-constant reservoir pressure boundary condition (see Figure 19), caused the pipeline simulator to predict a faster warmup in the riser and, hence, the system predicted that the safe operating temperature (SOT), say 10 degC above hydrate formation temperature, was reached on 3/27/2007. This safe operating temperature limit is used as guidance by the operator and, therefore, the operator would have

switched off methanol injection on 3/27/2007. In actuality, the tuned VMS data shows that SOT was not reached until 3/31/2007 after well 2 was started up. Thus a tuned model is important for safe operations and does help in reducing operational cost.

The integrated system also comes with standard look-ahead/what-if forecast modules. The common modules are (i) cool-down forecast, which starts from the current state and predicts the time left to reach certain pre-configured alarm conditions such as No-touch time, Light-touch time, and time-to-hydrate formation condition; (ii) warm-up forecast, which starts from the current state and can simulate a shutdown followed by startup till the conditions within the pipeline reaches the SOT limit; and (iii) hot-oil circulation, which provides the hot-oil volume required to warm-up the system. A typical operator advisory window is shown in Figure 21.

Since the real time systems – VMS for the wells and the pipeline simulator for the flowlines – are calibrated and tuned to field conditions, and the forecast modules use the same underlying physical models, a high degree of accuracy is achieved in these forecasts.

## **Field Example of Integrated Applications**

### **Restriction Detection**

Here, we discuss a specific application that we deployed for a major oil & gas producer in the Southern North Sea. The operator had issues with hydrate blockages occurring in their infield flowlines, which transport gas, condensate, and water. So, they approached us to install a system that would provide early detection warnings in case of a restriction, presumably due to hydrates, in their infield flowlines.

The network topology on which the application was deployed is shown in Figure 22. Flow from the subsea manifolds (A, B, C, D, and F) is commingled with production from (unmanned) platform (E and G) wells and transported to a manned platform (H), where processing facilities exist and water is separated, before being transported via export trunklines to the shore terminal. The commingled field production is measured only at platform H on the gas and liquid legs of two separators. The assets are distributed in water depths of 35–50 meters with well CGR's ranging from 3-4 bbl/MMscf and the WGR's ranging from 0.5-4 bbl/MMscf.

### **Approach**

The strategy that we agreed upon was that if we could predict the pressures in the infield pipelines, taking into account the continuous variations in flowrate and holdup in the flowlines, and tune it to match the field, then one could immediately notice when the field pressures start increasing due to a restriction (presumably due to hydrates) in the pipeline and deviating from model predictions.

The approach that we decided on was to deploy an integrated system -- VMS integrated with a real time pipeline flow simulator. VMS would be used to predict the real time well flowrates; from both the subsea and platform wells. These predicted flowrates would be used as the flow boundary condition for the three-phase transient pipeline model. The system would then continuously compare the model predicted pipeline pressures with the field measured pressures. If the field pressures start steadily (or abruptly) drifting away from the model predicted pressures, then it would indicate that something was amiss. If the field pressure is increasing, then it would indicate a restriction in the pipeline.

In order to make this approach work, one needed to accomplish two things: (i) VMS needed to accurately predict the well flow rates, and (ii) the pipeline model needed to accurately capture field conditions such as the pressure drop, temperature drop, and holdup variations in each flowline.

### **Challenges**

One of the key challenges was that these were old wells and usually operated with the choke wide open. Figure 23 shows typical field data for the pressure before the choke and pressure after the choke. As can be observed, there is no pressure drop ( $dP$ ) across the choke and a simple choke model cannot be used to predict the well flowrates. In addition, the resolution of the pressure instrumentation is  $\pm 1$  bar and, hence, any estimation based on a choke model would be hugely erroneous.

Hence, we had to rely on a wellbore flow model to estimate the well flowrates. There were inherent difficulties in using this approach. The first was that these are really old wells and as-built wellbore diagrams were not readily available. Secondly, key reservoir information and well inflow performance data were also difficult to obtain. Thirdly, there are no subsea well-test lines and only the platform wells could be routed to the test separator. Thus, well-test data and individual well composition data was not available for the subsea wells.

Configuring and tuning the well models turned out to be a challenging task. These wells are cycled – opened and closed on a periodic basis -- in order to allow the near-wellbore pressure to buildup. So, these wells have a high production rate when they are opened up which then quickly decays with time till the wells are shut-in; and the cycle repeats. Figure 24 shows the rapid decay in the wellhead temperature and pressure, indicative of declining flowrates. So, in order to model this behavior, we had to again incorporate a near-wellbore reservoir model that could mimic the near-wellbore pressure build up and subsequent decay.

The wellhead pressure instrumentation on almost all the wells is located between the wing valve and the choke valve. The normal mode of operation is a wide open choke; so gradual pressure decay is observed as shown in Figure 24. When the well is shut-in, both of these valves are closed and the wellhead pressure behaves similar to that of a shut-in flowline – pressure decreases as the fluid is cooled to ambient, as shown in Figure 25 (a). Hence, we were not able to record and analyze the wellhead pressure rise and deduce/tune the wellbore storage coefficient and skin factor.

### **Implementation**

A positive step that we took during project execution was to identify all the data that we needed in order to configure and tune our models. Once the data was identified, we configured and installed a system at site to collect this data. This allowed us to periodically analyze the field data, configure our models, and tune them to field conditions. One of the benefits of this was that we were able to convince the operators to not close the wing valve and let us record at least one sample data set for each wellhead pressure buildup during shut-in; a sample result is shown in Figure 25 (b). This information was critical in tuning VMS.

#### ***Performance***

Once we tuned the wells, we were able to get a good match between the predicted flow rates and the measured (commingled) flowrates at the production separators. Figure 26 shows that we were able to get a good match between the measured gas flowrates and the model predicted flowrates.

After tuning the well models, we were now able to accurately predict the three-phase flowrates going into the individual flowlines. Next step was to tune the pipeline flow models for pressures, temperatures, and holdup. Finally, we were able to get a good agreement between the field pressures and the model predicted pressures; see Figure 27. Now, we had a software model that accurately simulated the entire field and at this point, the system was ready to detect restrictions.

#### ***Key Lesson***

One of the key lessons we learned was that the emergency shutdown system could trigger a false blockage alarm. Figure 28 shows the difference between the measured pressure and the model predicted pressure at the platform E export conditions, i.e. flowline 5 inlet. It turns out that the emergency system tripped and the platform export ESD valve, which is downstream of the export pressure transmitter, tripped before the well master valve causing the export pressure to rise. The restriction detection system had the well master valve configured in its database but did not have the export ESD valve configured. Consequently, the model predicted pressures dropped when the wells were shut-in. The resulting error caused the system to send a blockage alarm.

It is not possible to account for each and every valve in the system and it only makes the system more complicated than necessary. The solution that we ended up preferring was not to send a blockage alarm when the wells are shut-in.

#### **Leak Detection**

We looked at the feasibility of using VMS for leak detection for a project in the Middle East. It was a complex network of pipelines fed by large number of wells, ninety (90) wells in total, all flowing into a couple of Gas Oil Separation Plants (GOSPs). Some of the wells are offshore in shallow water while most were onshore. The crude had sufficiently high concentration of H<sub>2</sub>S and these buried pipelines were going through dense population areas. Hence, the need was not only to detect sufficiently small leaks but to also locate the leaks accurately. One of the solutions explored was to install H<sub>2</sub>S sniffers all along the pipeline, but this is an expensive solution. Another approach was to put in a physical multiphase meter for each well and use a model-compensated software-based leak detection technique, but this also turns out to be quite expensive. Hence, we were approached to investigate the leak detection and location sensitivity that could be achieved by using a virtual metering system coupled to a model-compensated software-based leak detection system.

We looked at three distinct pipeline networks, with roughly thirty (30) wells each, transporting three different grades of crude – with solution GORs ranging from 330 to 1300 and fluid APIs ranging from 29 to 42. One of the networks is shown in Figure 29.

#### ***Challenges***

One of the challenges in detecting leaks in these networks was that the operating pressures were low – the heavier crude was arriving at the GOSP at approximately 35 psig while the lighter crude was arriving at the GOSP at 135 psig. There were no flow measurement anywhere in the system; the only measurements were downstream of the production traps at the GOSPs. Thus, even if a leak is detected using a model-compensated mass balance technique, the difficulty would still remain in locating the leak in this interconnected network.

#### ***Approach***

For the feasibility study, we created a model of the entire network (including the wells) using a standard multiphase flow design tool. We used this design tool to simulate/generate the field response that would result in the event of a leak. We simulated leaks of various sizes at various locations within the network – at steady state and during transient events such as rampups and rampdowns. The data from the design tool was superimposed with random noise to simulate responses closer to actual field conditions. This data was fed to our virtual metering system integrated with a dynamic pipeline simulator. If the virtual metering system correctly predicts the well flowrates and the pipeline simulator accurately models the field pressures, then in the event of a leak, one would detect a mass imbalance at the GOSPs as well as pressure discrepancies within the pipeline network between the field values and the model predictions. These error signals can be analyzed to detect whether a leak has occurred and where it is located.

Table 1 summarizes the result of this feasibility study. For this low pressure network, the lowest detectable leak size was 30 mm and it took 2-3 hours to detect these small leaks. Larger leaks, of 120 mm size, could be detected fairly quickly within 10-20 minutes. Figure 30 (a) shows the variation in leak detection time as a function of leak size. There is evidently a lot of scatter in the detection times for small leaks. That is because the detection times are sensitive to the location of the leak – whether the leak is at either end of the pipe branch, i.e. close to the location of a pressure transmitter, or whether it is in the middle of the pipe branch away from a pressure transmitter.



Figure 31 shows a comparison of the (simulated) field data, when a 60 mm leak is initiated at  $t = 20,000$  sec in the network (in branch 6), and the model predictions. Note, a 60 mm leak size does not result in a large leak rate (in % of operating flowrate) because the network is at a low pressure. It is difficult to look at the raw signals and deduce that there has been a leak. If you look at the errors, i.e. model predicted flowrates minus measured flowrates, and its moving averages, then you can notice the imbalance in the liquid volume rates almost immediately after the leak is initiated at  $t=20,000$  sec. The imbalance in the gas volume rates takes longer to propagate through the network and is noticeable only 5-6 hours after the leak.

In the event of a leak in this interconnected network, the pressures drop everywhere and it is difficult to figure out the leak location by looking the pressure signals; especially when the scan rate is of the order of ten to twenty seconds. Another factor to consider is that a lowered pipeline pressure will cause the wells to see a reduced back pressure and produce more. By breaking the pipeline network model into discontinuous pressure segments, without breaking the flow continuity, and using available field pressures to supply the boundary conditions, one is able to observe different pressure error patterns and, thereby, locate the leak. Figure 32 shows the pressure response in the field for the 60 mm leak in branch 6. As a result of using the right boundary conditions, the pressure error (model pressure minus field pressure) in branch 6 goes up as expected in the event of a leak, while the pressure errors in the other branches stay almost unchanged. Further analysis of the pressure-time response is performed to figure the exact location of the leak. Figure 30 (b) shows the variability in locating the leaks depending on where the leak is located within the network. The errors in locating leaks also depend on the leak size - smaller leaks are harder to locate because the pressure signals were weaker.

**Conclusions**

Virtual metering systems have been in operation for more than a decade and can now be considered to be a mature technology. Over the years, VMS has developed into a robust technology that can overcome real-life installation issues such as data unavailability, communications problems, data degradation, and system maintainability over the entire field life. These systems combine multiple methods to provide a robust estimate with the lowest overall uncertainty. These uncertainties are used to back-allocate the reconciled production to the wells. These systems are also equipped with smart logic to detect instrument failures and sudden changes in field conditions and provide an early warning to the operator.

Certain best practices if followed during project execution can lead to a successful VMS installation. First, the FAT should be conducted with actual tags loaded on an actual test system (software plus hardware) that replicates the field system as closely as possible. Whenever possible, VMS should obtain data directly from the tag server or a data server that is feeding the control room and/or other critical applications. This ensures that any communications problems will be noticed immediately. VMS key results and alerts should be displayed on the SCADA/DCS screens; this prompts both the operator and vendor to service the system promptly. To this end, remote access goes a long way in enabling the vendor to provide prompt service and assistance and check system status on a frequent basis. Design data and assumptions should be checked and validated during commissioning and, whenever possible, the system should be calibrated at both high and low choke settings. Historical data suggests that monthly reconciliation factors as low as 2-3% can be achieved by following these guidelines.

These systems can easily be integrated with real time pipeline simulators to offer a wide range of fit-for-purpose solutions. These range from standard forecasting tools for flow assurance guidance on issues such as cool-downs and warm-ups to complex solutions such as hydrate restriction detection and leak detection. Since these real time systems are calibrated to the actual field condition, these solutions provide results with a high degree of accuracy.

**Acknowledgments**

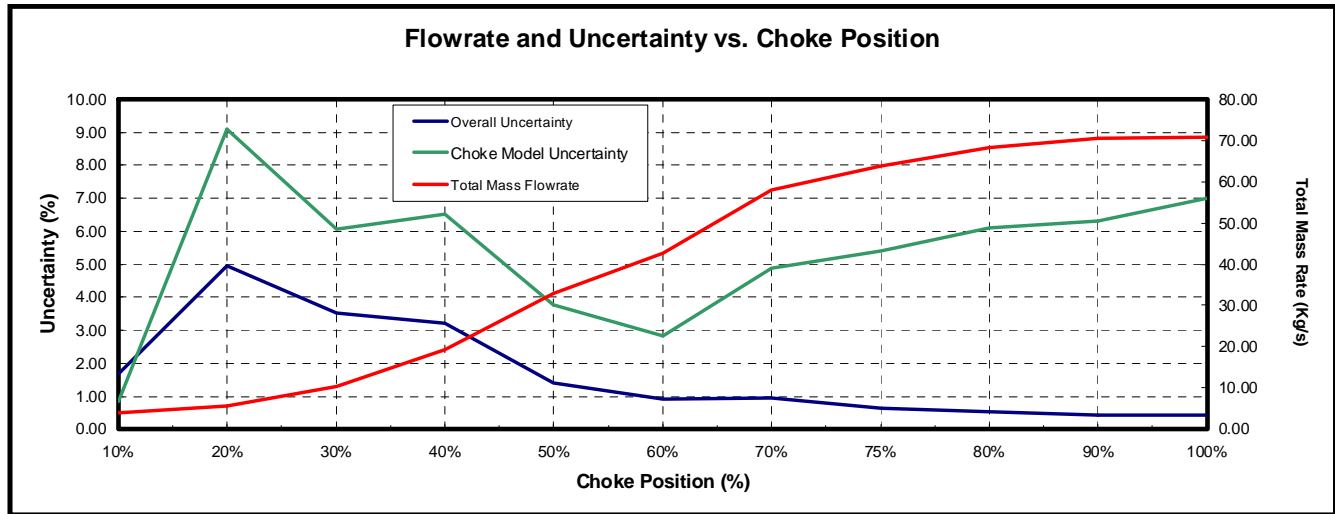
The authors wish to thank Saiful Molla for his assistance in preparing this manuscript and for all the long hours spent just before the deadline. Thanks also to Pradeep Dhoorjaty and Danny Golczynski for their help in reviewing the paper.

**References**

Haldipur, P., Parthasarathy P., and Erickson D., (2007). Case Study: Multiphase Flow Simulation Technology to Plan Pigging Programs, Oil & Gas Eurasia, No. 6, June 2007.  
 Parthasarathy, P., Haldipur, P., and Erickson, D., (2007). Real-time Pipeline Monitoring, Pipeline and Gas Technology, May 2007.  
 Llave, S. (2005). Case History: Lessons learned in delivering real-time, on-line pipeline and asset management systems in Southeast Asia, PetroMin Pipeliner, May, 2005.  
 Picart, P. and Llave, S. (2004). Virtual System provides reliable multiphase metering from Malampaya wells, Oil & Gas Journal, May 2004.  
 Scott, S. L. and Barrufet, M. A. (2003). Worldwide Assessment of Industry Leak Detection Capabilities for Single & Multiphase Pipelines. Project Report Prepared for the Minerals Management Service under the MMS/OTRC Cooperative Research Agreement 1435-01-99-CA-31003.

**Table 1: Leak sensitivity summary for the crude oil networks**

Subsystem	Minimum Detectable Leak Size (mm)	Average Detection Time for Smallest Detectable Leak (min)	Average Leak Detection Time for Large Leaks (min)	Mean Error in Leak Location (km)
GOSP-A	30	180	8	2.24
GOSP-B	30	110	20	1.92



Results

Flowrate Methods	Choke Position(%)										
	10%	20%	30%	40%	50%	60%	70%	75%	80%	90%	100%
<b>Best Estimated Flowrate (kg/s)</b>	<b>4.00</b>	<b>5.66</b>	<b>10.42</b>	<b>19.24</b>	<b>32.89</b>	<b>42.56</b>	<b>58.12</b>	<b>63.96</b>	<b>68.30</b>	<b>70.37</b>	<b>70.89</b>
<b>Overall Uncertainty (%)</b>	<b>1.69</b>	<b>4.94</b>	<b>3.52</b>	<b>3.21</b>	<b>1.41</b>	<b>0.91</b>	<b>0.95</b>	<b>0.63</b>	<b>0.52</b>	<b>0.42</b>	<b>0.43</b>
<b>Individual Method Uncertainties</b>											
1. Reservoir and Manifold Pressures (%)	10.94	13.22	7.17	7.65	3.52	2.35	3.67	1.75	1.32	1.05	1.05
2. Reservoir and After Choke Pressures (%)	10.88	13.19	7.16	7.67	3.56	2.41	3.83	1.95	1.54	1.33	1.33
3. Reservoir and Before Choke Pressures (%)	107.91	78.70	33.97	14.86	4.73	2.91	1.66	1.38	1.22	1.20	1.12
4. Bottom Hole and Manifold Pressures (%)	10.91	13.28	7.22	7.80	3.69	2.42	4.14	1.74	1.34	0.78	0.78
5. Bottom Hole and After Choke Pressures (%)	10.98	13.22	7.21	7.83	3.69	2.49	4.32	1.98	1.71	1.30	1.59
6. Bottom Hole and Before Choke Pressures (%)	110.48	87.40	38.61	10.62	3.80	1.96	1.21	1.06	0.83	0.76	0.75
7. IPR Model (%)	117.83	81.07	35.29	14.72	6.35	4.14	2.44	2.06	1.85	1.76	1.74
<b>8. Choke Model (%)</b>	<b>0.83</b>	<b>9.09</b>	<b>6.08</b>	<b>6.50</b>	<b>3.77</b>	<b>2.81</b>	<b>4.90</b>	<b>5.40</b>	<b>6.10</b>	<b>6.30</b>	<b>7.00</b>
9. Jumper Model (%)	468.96	318.07	119.68	42.63	15.63	9.54	5.32	4.43	3.99	3.79	3.74
<b>Individual Method Flowrates</b>											
1. Reservoir and Manifold Pressures (kg/s)	3.76	4.34	10.35	19.12	32.81	42.48	58.01	64.36	68.15	70.26	70.74
2. Reservoir and After Choke Pressures (kg/s)	3.76	4.34	10.35	19.12	32.81	42.48	58.02	64.35	68.16	70.26	70.74
3. Reservoir and Before Choke Pressures (kg/s)	8.10	8.90	10.37	19.24	32.89	42.53	57.98	62.92	68.17	70.15	70.73
4. Bottom Hole and Manifold Pressures (kg/s)	3.76	4.34	10.36	19.14	32.84	42.56	58.11	64.47	68.44	70.51	71.00
5. Bottom Hole and After Choke Pressures (kg/s)	3.76	4.34	10.36	19.14	32.86	42.57	58.12	64.48	68.47	70.55	71.20
6. Bottom Hole and Before Choke Pressures (kg/s)	9.10	9.60	12.41	20.15	33.25	42.75	58.33	62.66	68.44	70.47	70.95
7. IPR Model (kg/s)	3.62	4.25	10.29	19.12	32.81	42.50	58.04	64.35	68.20	70.26	70.74
8. Choke Model (kg/s)	3.64	4.27	10.34	19.11	32.81	42.51	58.07	68.85	68.29	70.48	71.07
9. Jumper Model (kg/s)	3.33	3.91	9.43	17.65	30.62	40.05	55.58	62.39	66.17	68.37	68.89

Figure 1: VMS flowrate and uncertainty estimates as a function of choke position

Flowrate Methods	Data Quality (%)	
	Healthy	Unhealthy (Except Before Choke Pressure and Temperature)
<b>Best Estimated Flowrate (kg/s)</b>	<b>63.96</b>	<b>62.29</b>
<b>Best Estimated Uncertainty (%)</b>	<b>0.63</b>	<b>2.08</b>
<b>Individual Method Uncertainties</b>		
1. Reservoir and Manifold Pressures (%)	1.75	350.00
2. Reservoir and After Choke Pressures (%)	1.95	350.00
3. Reservoir and Before Choke Pressures (%)	1.38	1.69
4. Bottom Hole and Manifold Pressures (%)	1.74	350.00
5. Bottom Hole and After Choke Pressures (%)	1.98	350.00
6. Bottom Hole and Before Choke Pressures (%)	1.06	1.78
7. IPR Model (%)	2.06	3.67
8. Choke Model (%)	5.94	350.00
9. Jumper Model (%)	4.43	350.00
<b>Individual Method Flowrates</b>		
1. Reservoir and Manifold Pressures (kg/s)	64.36	62.92
2. Reservoir and After Choke Pressures (kg/s)	64.35	62.92
3. Reservoir and Before Choke Pressures (kg/s)	62.92	62.92
4. Bottom Hole and Manifold Pressures (kg/s)	64.47	62.92
5. Bottom Hole and After Choke Pressures (kg/s)	64.48	62.92
6. Bottom Hole and Before Choke Pressures (kg/s)	62.66	62.92
7. IPR Model (kg/s)	64.35	60.00
8. Choke Model (kg/s)	68.85	90.00
9. Jumper Model (kg/s)	62.39	0.00

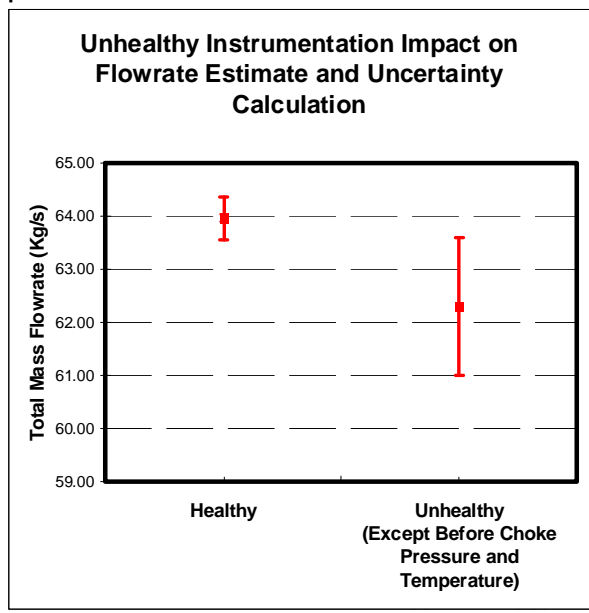


Figure 2: Estimated VMS flowrate when all instrumentation fails except one before choke pressure & one before choke temperature sensor

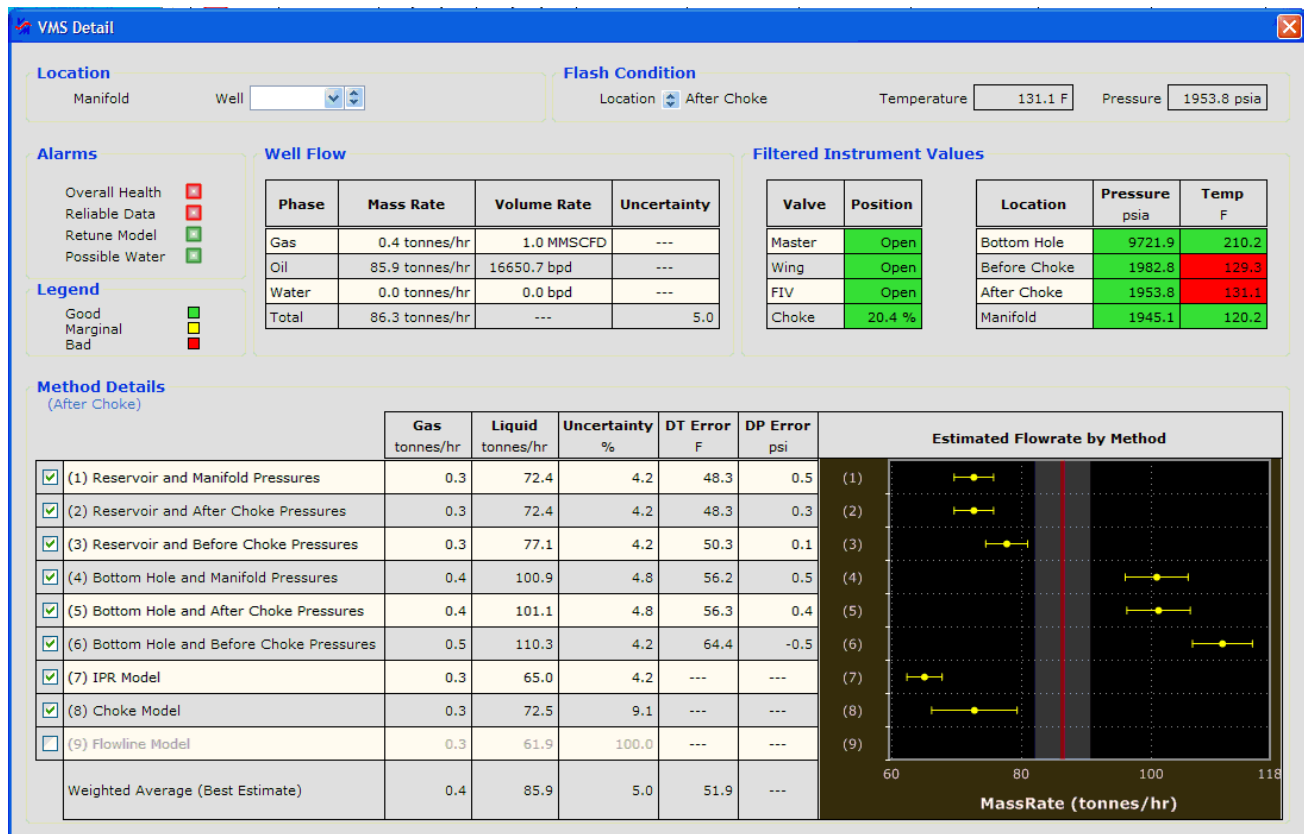


Figure 3: VMS screen with the various method calculations and surveillance information

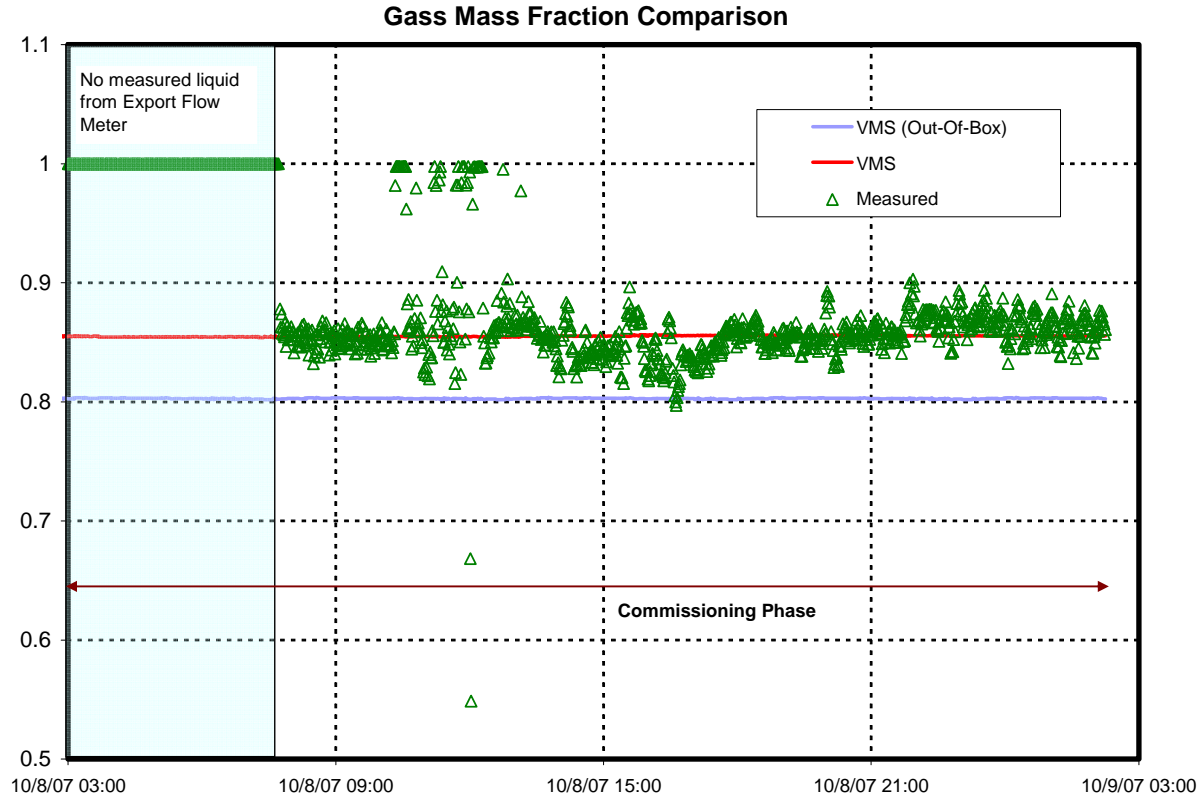


Figure 4: Predicted vs. Measured Gas Mass Fraction – during (untuned) commissioning and (tuned) post-commissioning

### Gas Mass Flowrate Comparison

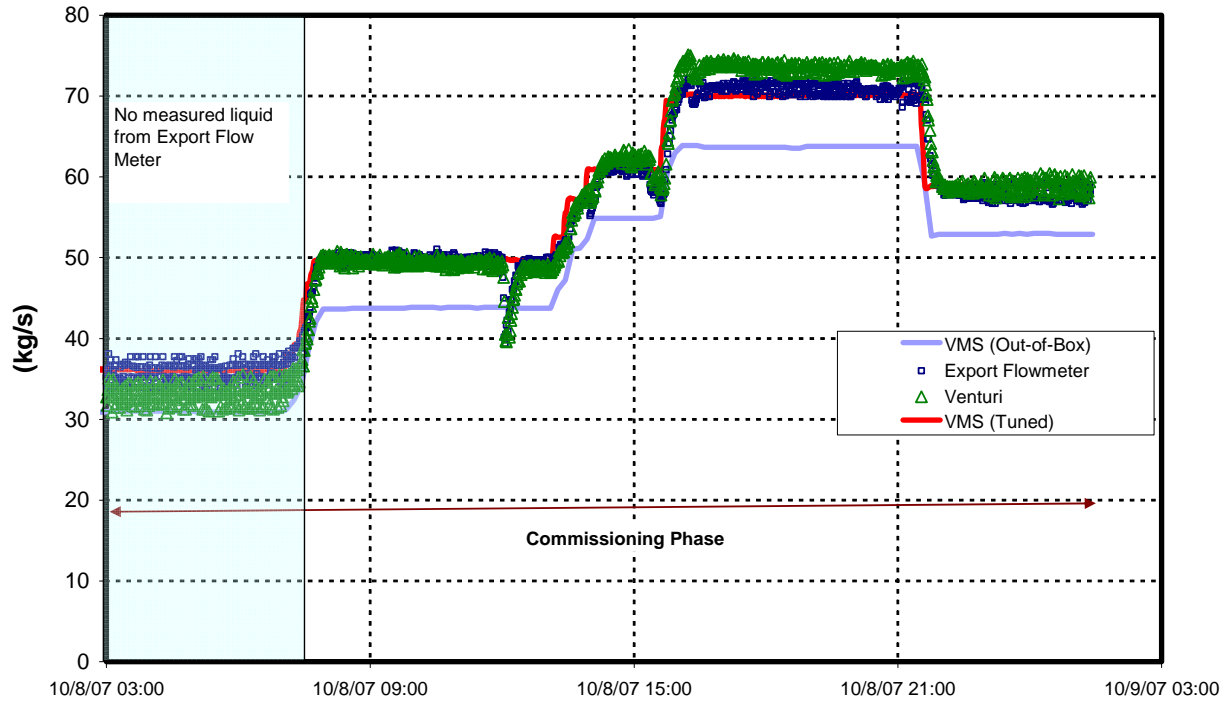


Figure 5: Comparison of Gas Mass Rate predictions before tuning (out-of-the-box) and after tuning VMS

### Liquid Mass Flowrate Comparison

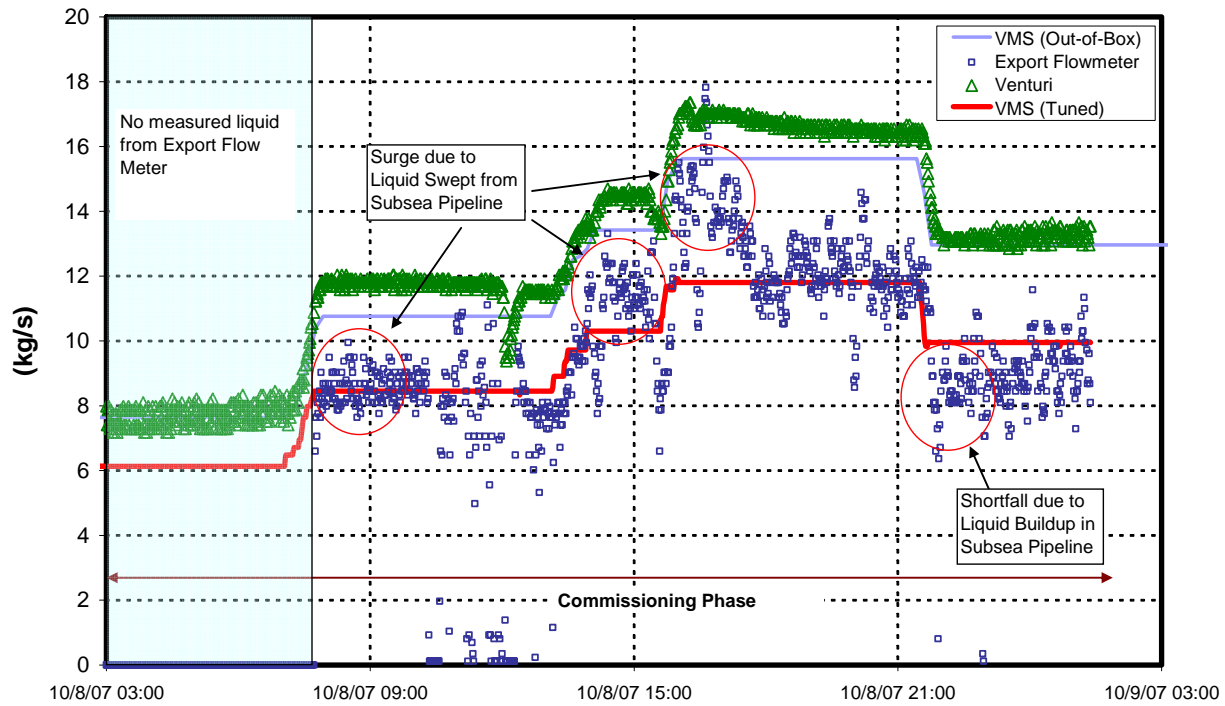


Figure 6: Comparison of Liquid Mass Rate predictions before tuning (out-of-the-box) and after tuning VMS

### Total Mass Flowrate Comparison

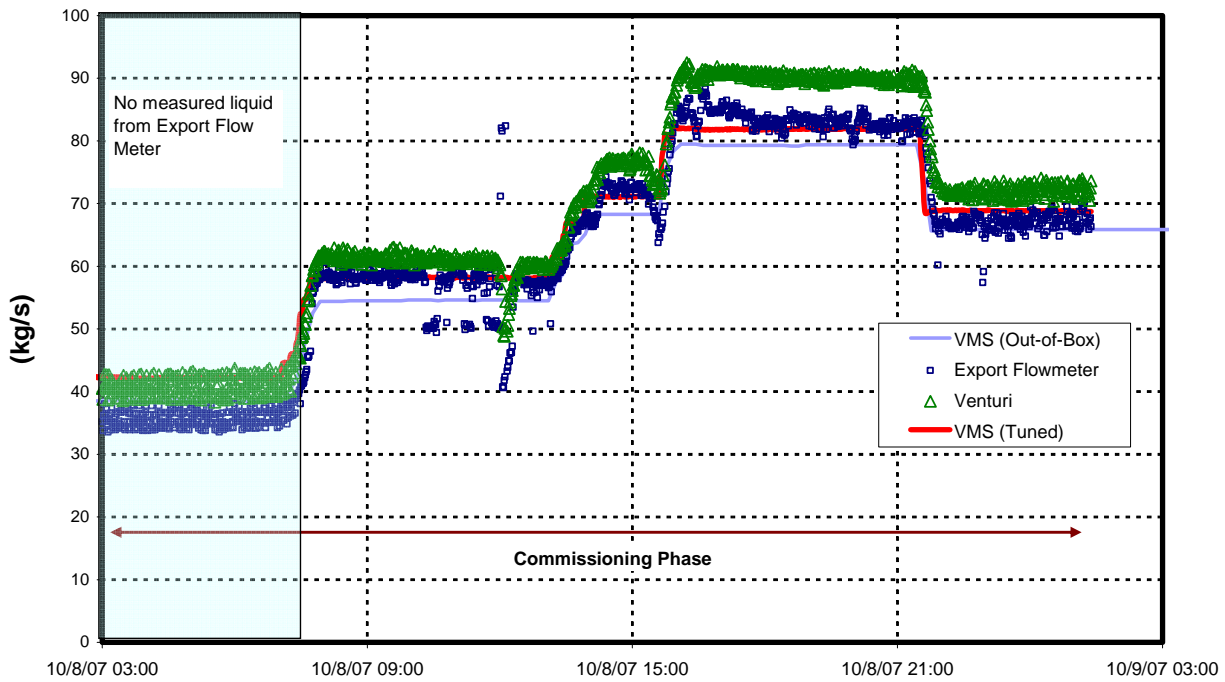


Figure 7: Comparison of Total Mass Rate predictions before tuning (out-of-the-box) and after tuning VMS

### Validation of Well 2 by Difference: Gas Mass Rates

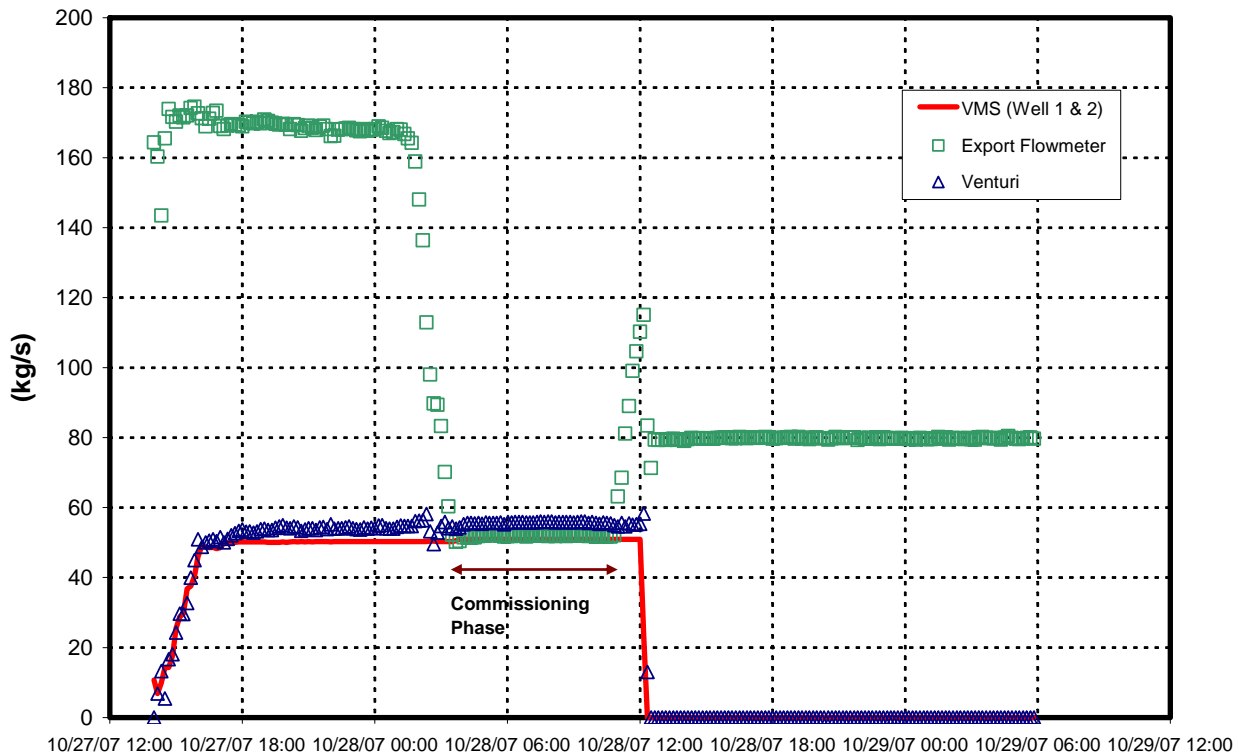


Figure 8: Gas Mass Rate comparison after tuning by difference

### Validation of Well 2 by Difference: Liquid Mass Rates

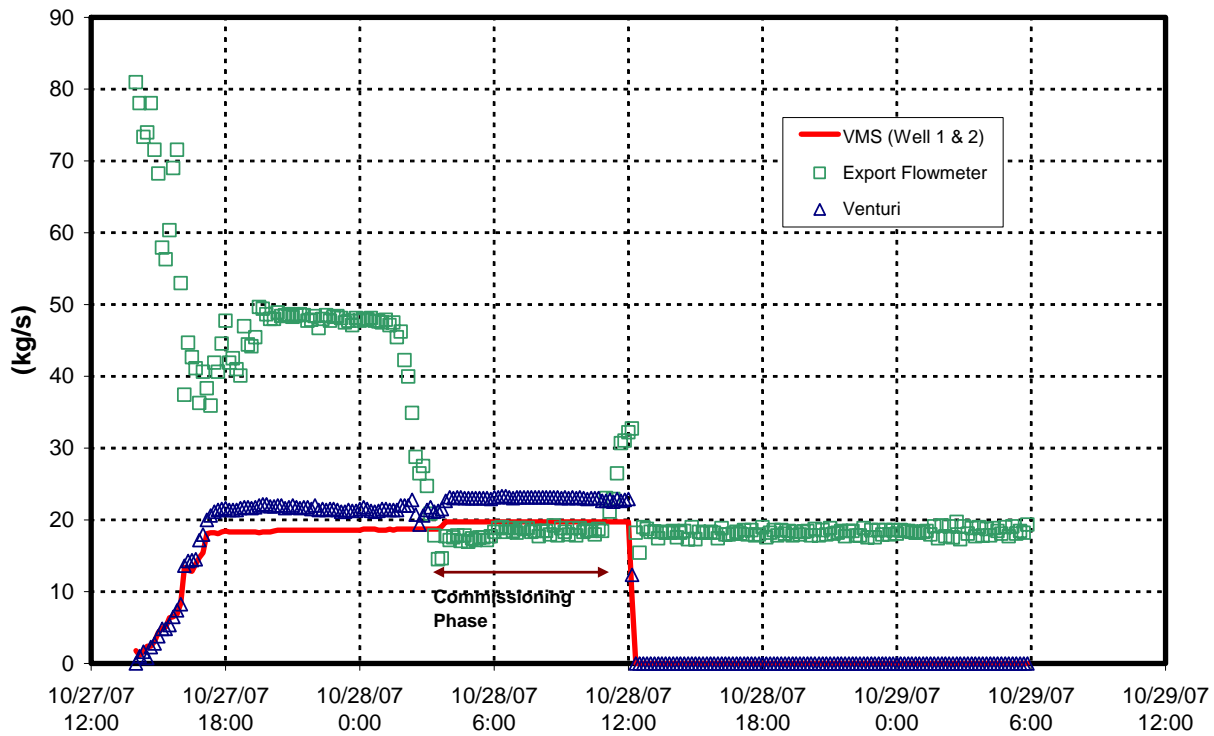


Figure 9: Liquid Mass Rate comparison after tuning by difference

### Well 2 Validation Bottom Hole Pressure Prediction

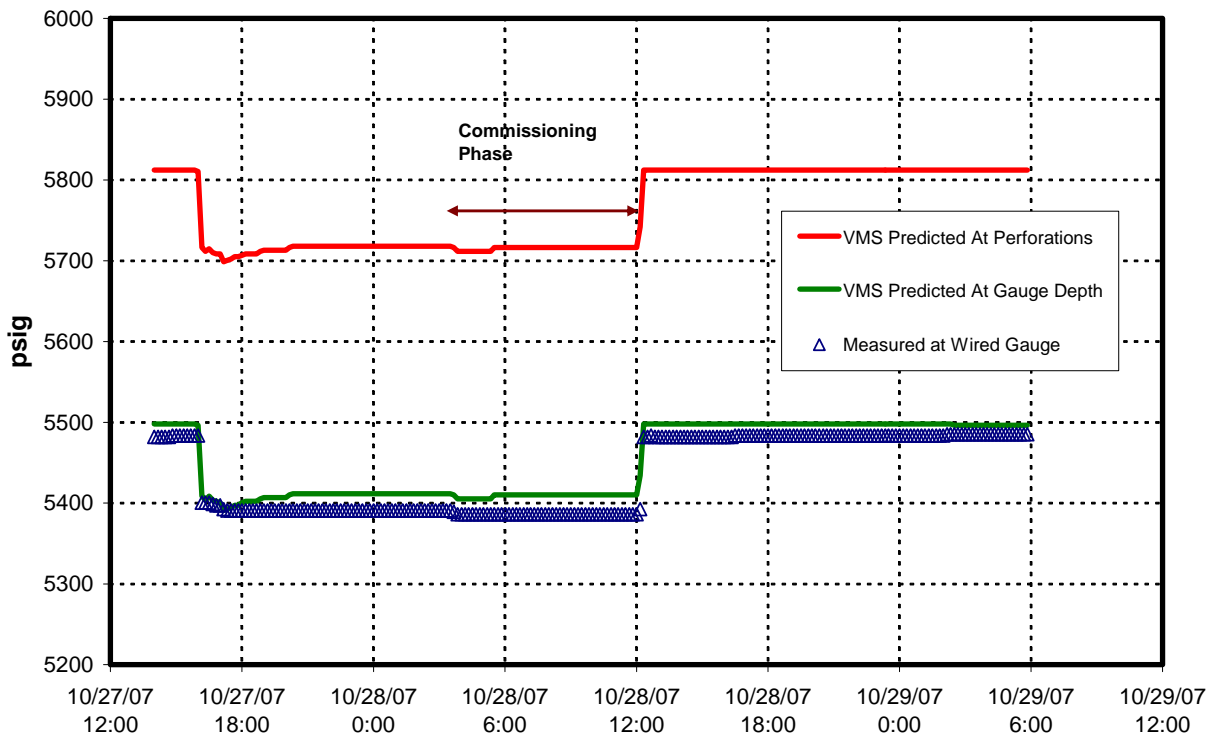


Figure 10: Comparison of model predicted pressure at the downhole gauge location vs. the measured downhole pressure

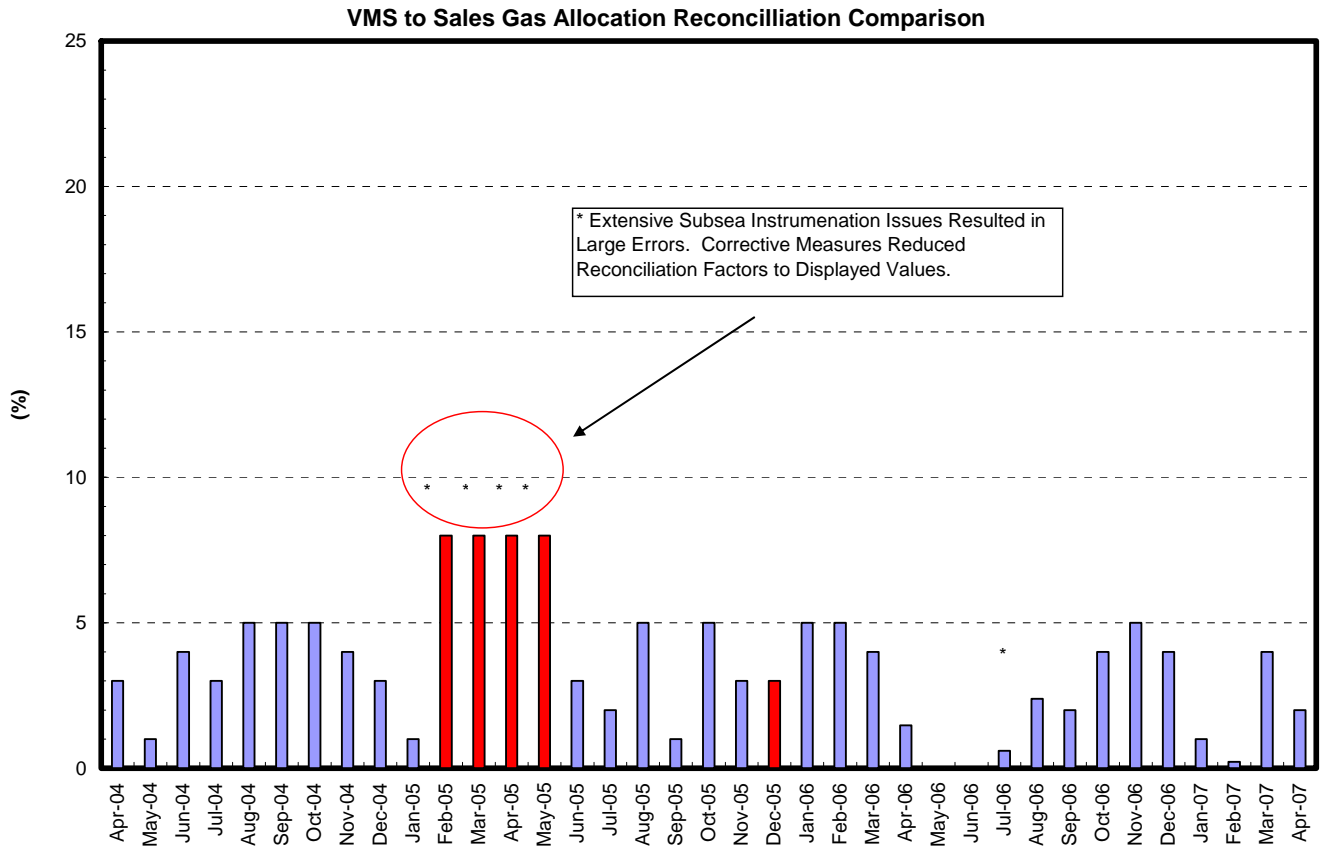


Figure 11: Historical Monthly reconciliation factors for a five (5) well VMS installation

### Well C Flowing Wellhead Pressure Data

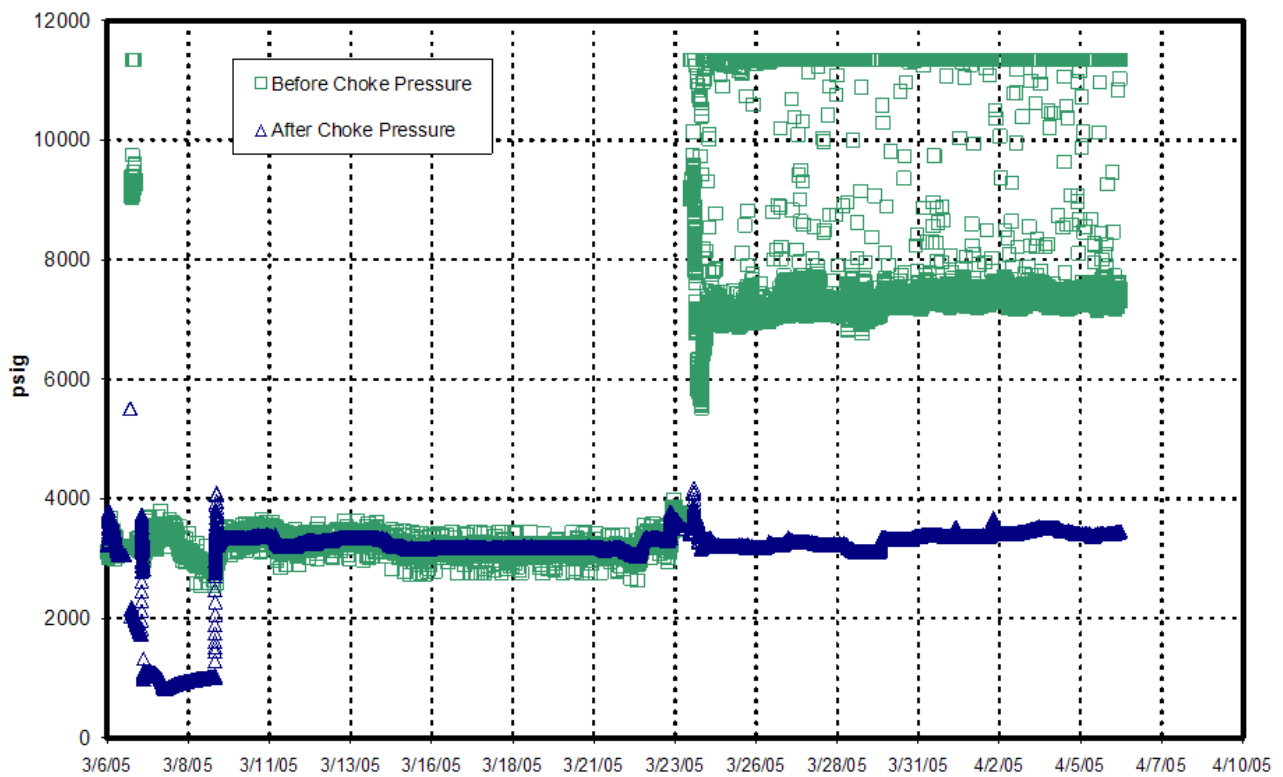


Figure 12: Instrument errors and data dropouts in Q2 of 2005

### MeOH Concentration

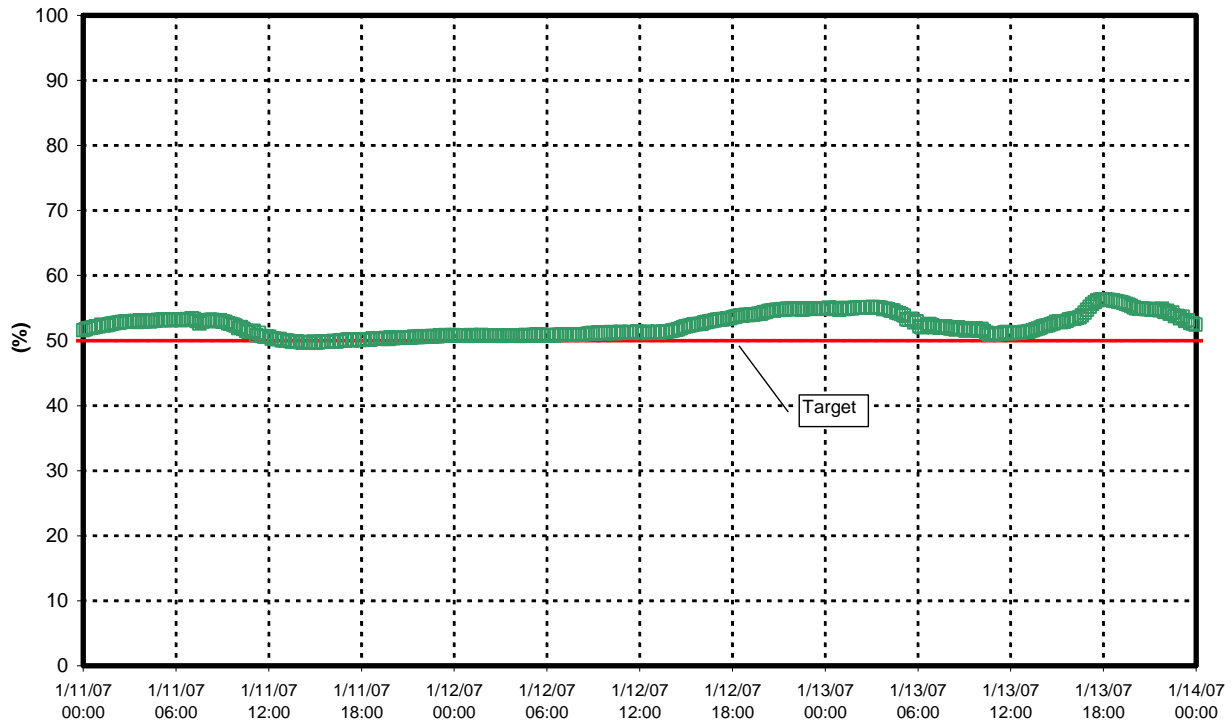


Figure 13: Measured methanol concentration at the platform

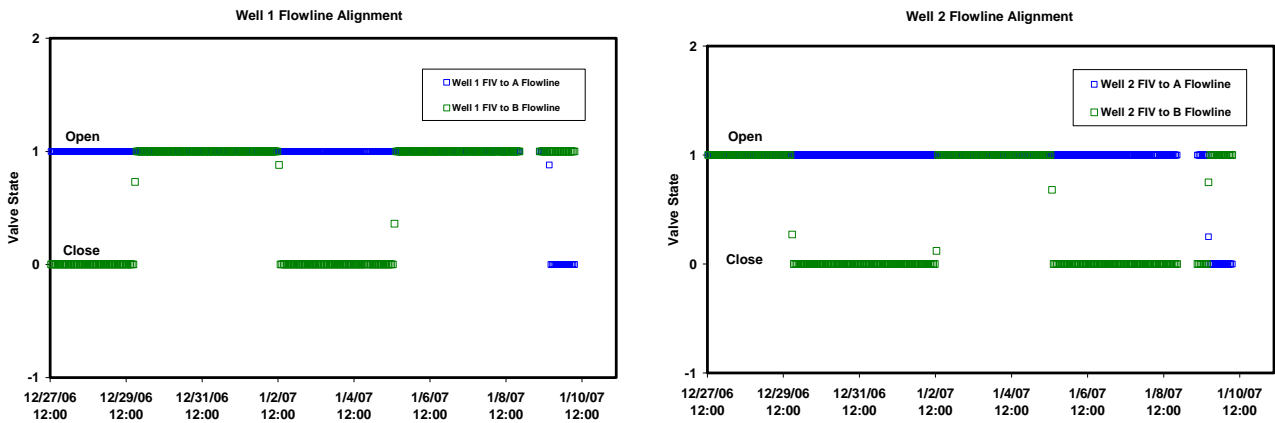


Figure 14: Flip-flopping data received for the FIV states which control the well alignment to the flowline

Well Overview

Current Mode For Subsea Well Alignment is Manual

### Well Overview at Well Head Conditions

Valve Alignment

Well	Choke	Master	Wing	SCSSV	DHP bara	DHT F	THP bara	THT F	Gas MMSCFD	Black Oil bpd	Water bpd	Pipeline	Separator	Separator Pressure bara
W1	100.0 %	✖	✖	✔	618.0	171.6	219.6	40.2	0.000	0.0	0.0	A Line	A	47.6
W2	24.8 %	✔	✔	✔	712.2	204.0	327.5	140.0	3.273	8816.4	143.3	B Line	B	43.9
W3	98.5 %	✔	✔	✔	512.9	199.4	157.0	154.6	17.681	15752.0	194.7	A Line	A	47.6
FW4	0.0 %	✖	✔	✔	0.0	-459.7	0.0	-459.7	0.000	0.0	0.0	--	-	0.0

Figure 15: Summary screen showing the well and flowline alignments



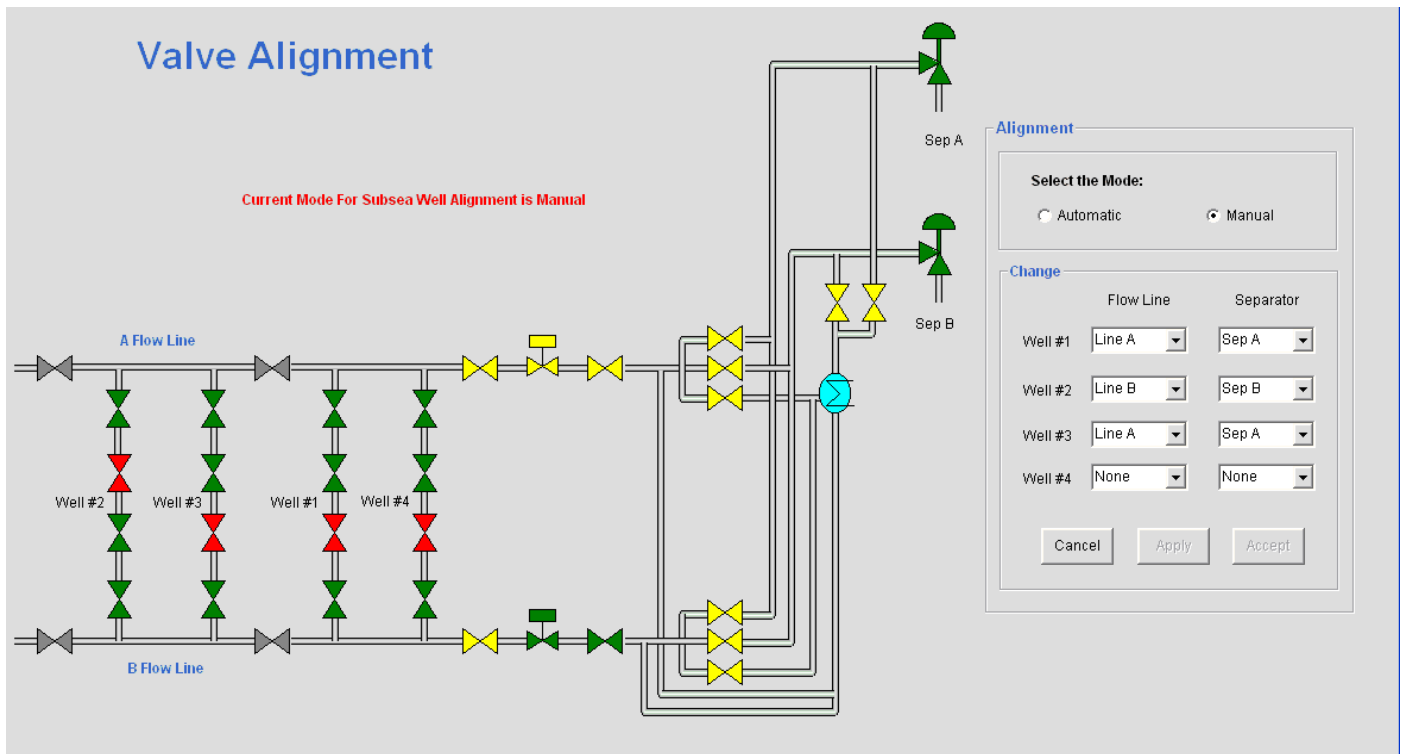


Figure 16: Detailed screen showing the valve signal conditions with manual override entry for the flow alignment

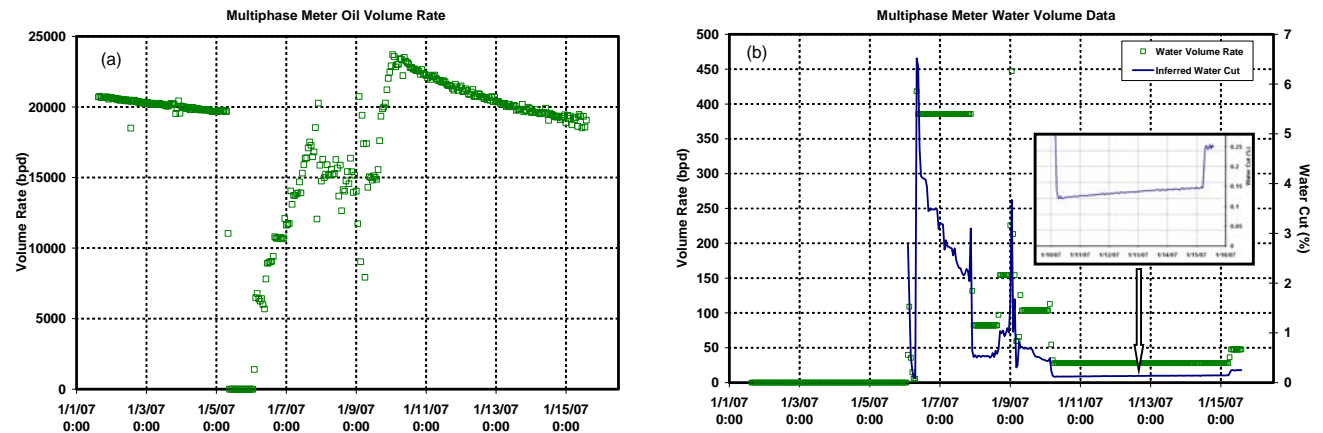


Figure 17: (a) Oil volume rate, and (b) water volume rates and inferred water cut, based on measurements from the topside multiphase meter

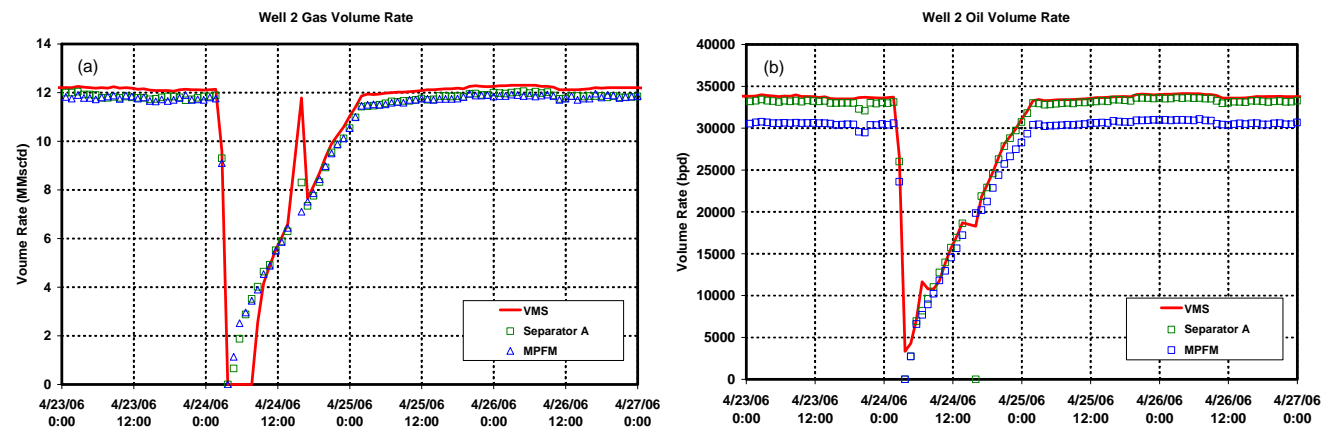


Figure 18: (a) Gas volume rate, and (b) oil volume rate, VMS (tuned) predictions for well 2 compared to production separator measurement and topside physical multiphase meter measurement

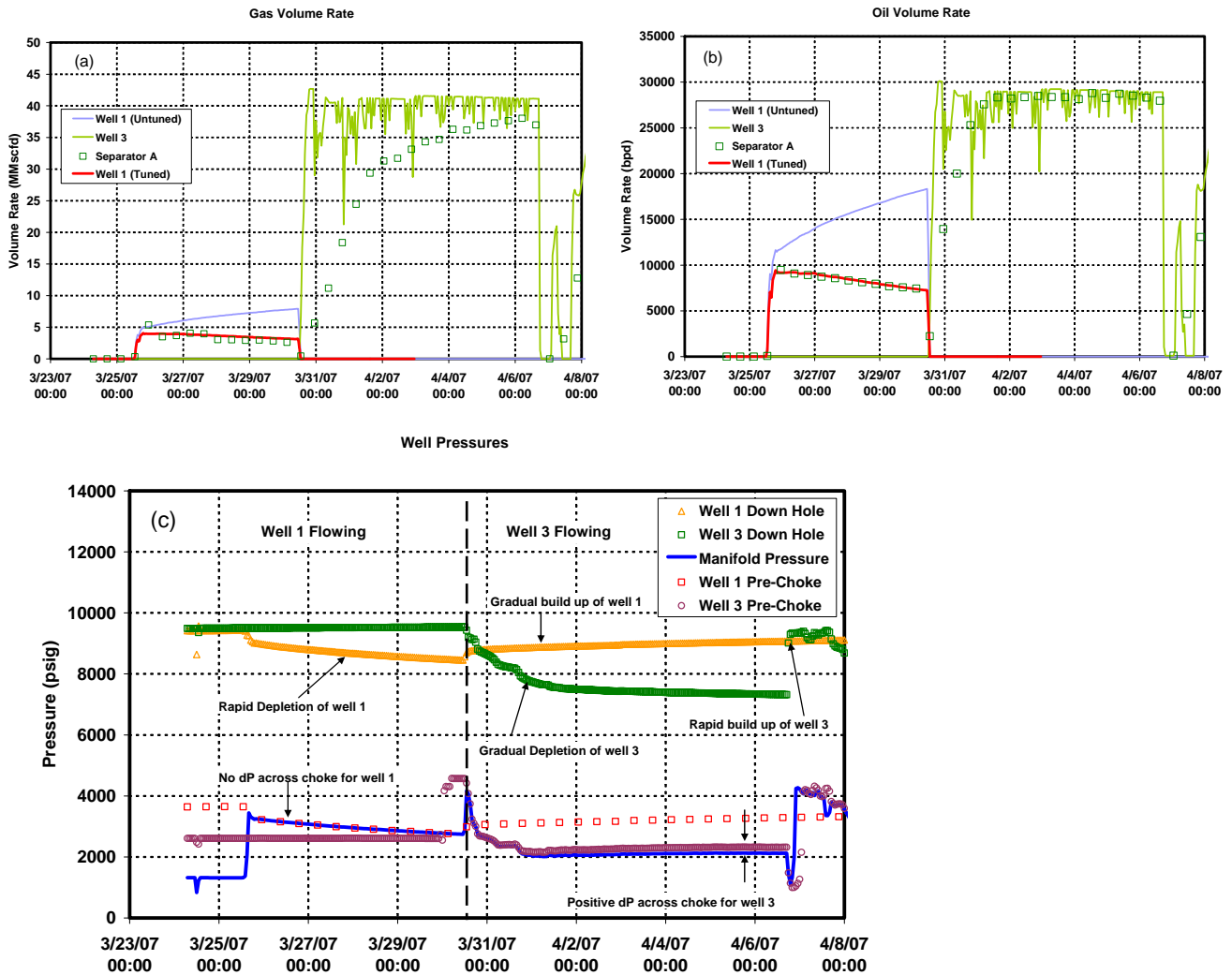


Figure 19: VMS predictions for (a) gas volume rate and (b) oil volume rate comparison for well 1 before (untuned) and after (tuned) incorporating a near-wellbore reservoir model; (c) startup and shutdown pressure data for well 1 & well 3

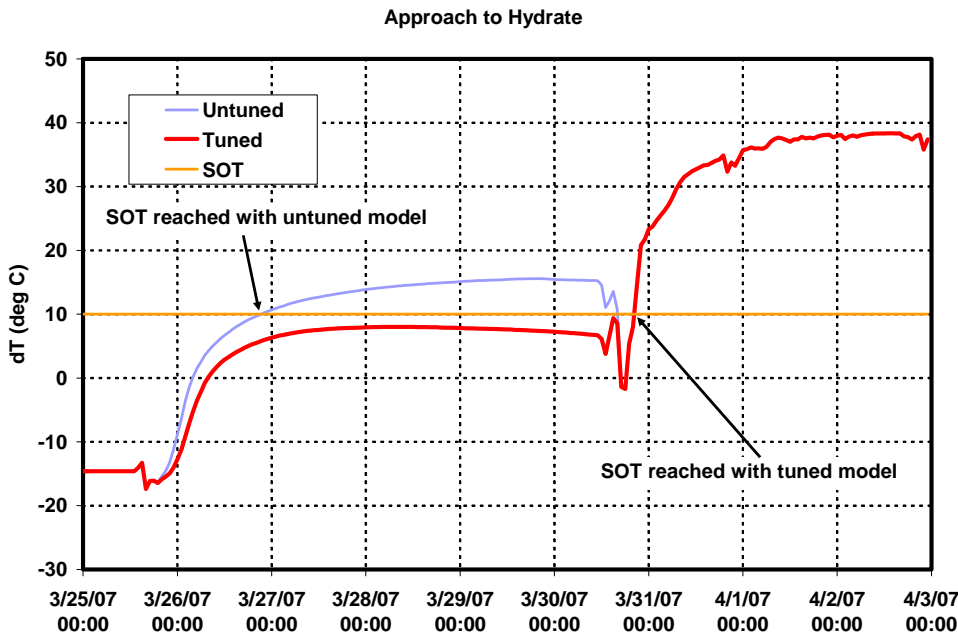


Figure 20: Comparison of pipeline warmup predictions before (untuned) and after (tuned) incorporating a near-wellbore reservoir model for well 1

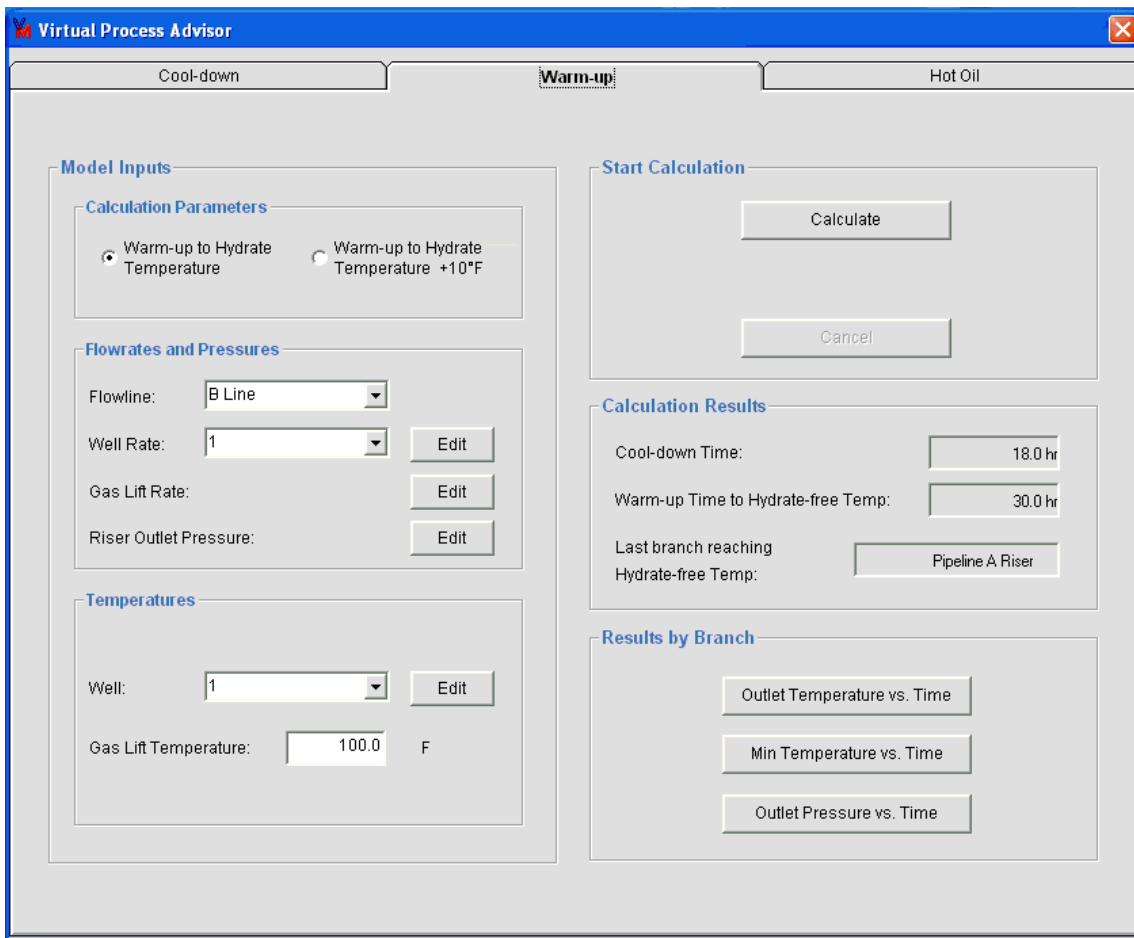


Figure 21: Process Advisor input window for Cool-downs, Warm-ups, and Hot-Oil Circulation

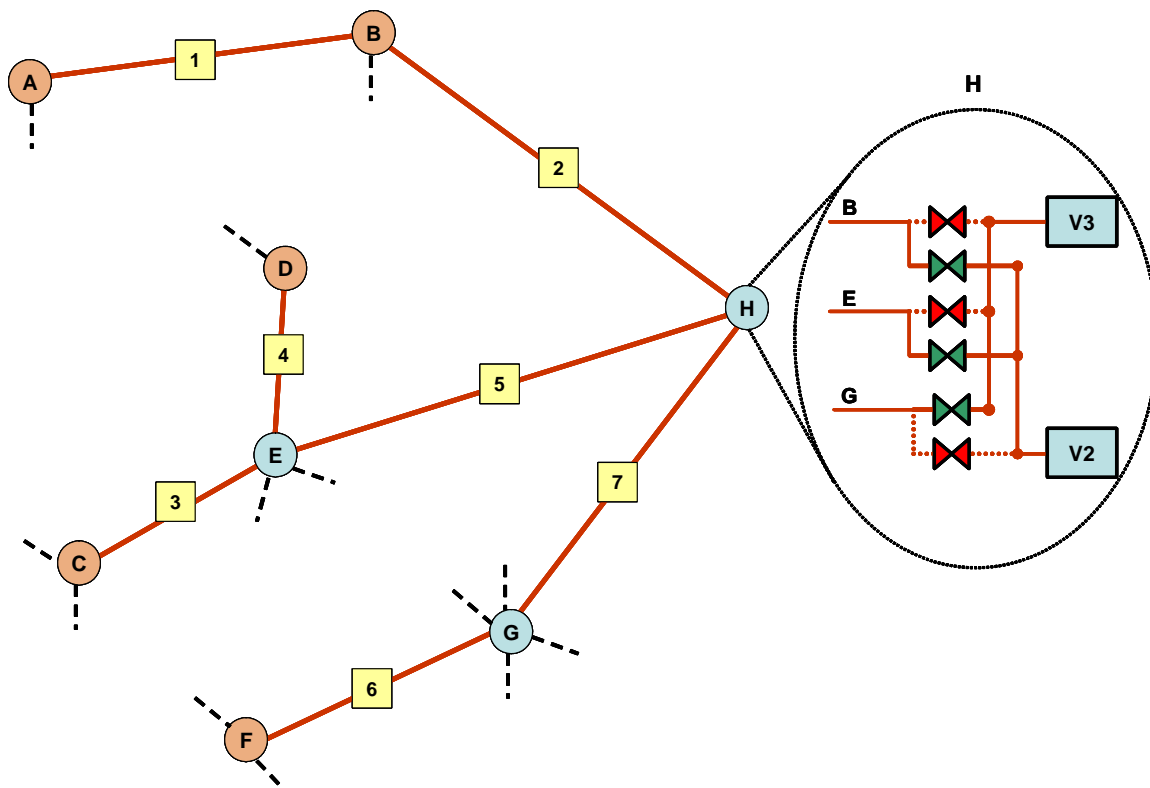


Figure 22: Network Topology for the infield flowlines in the Southern North Sea

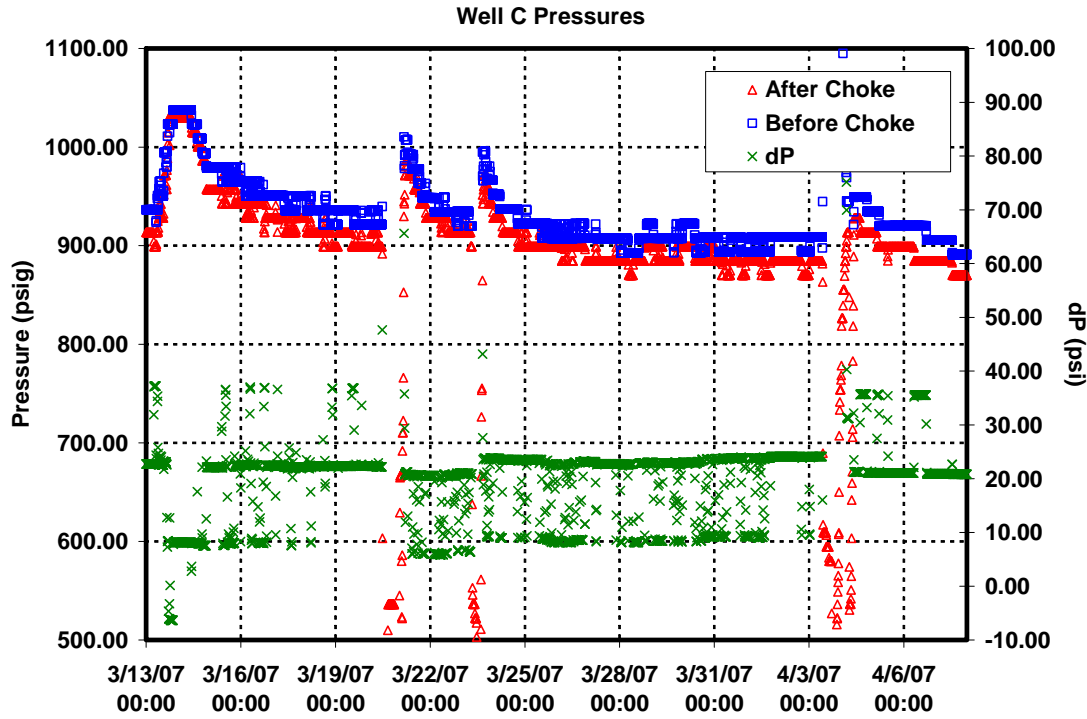


Figure 23: Typical pressure data across the choke for well C

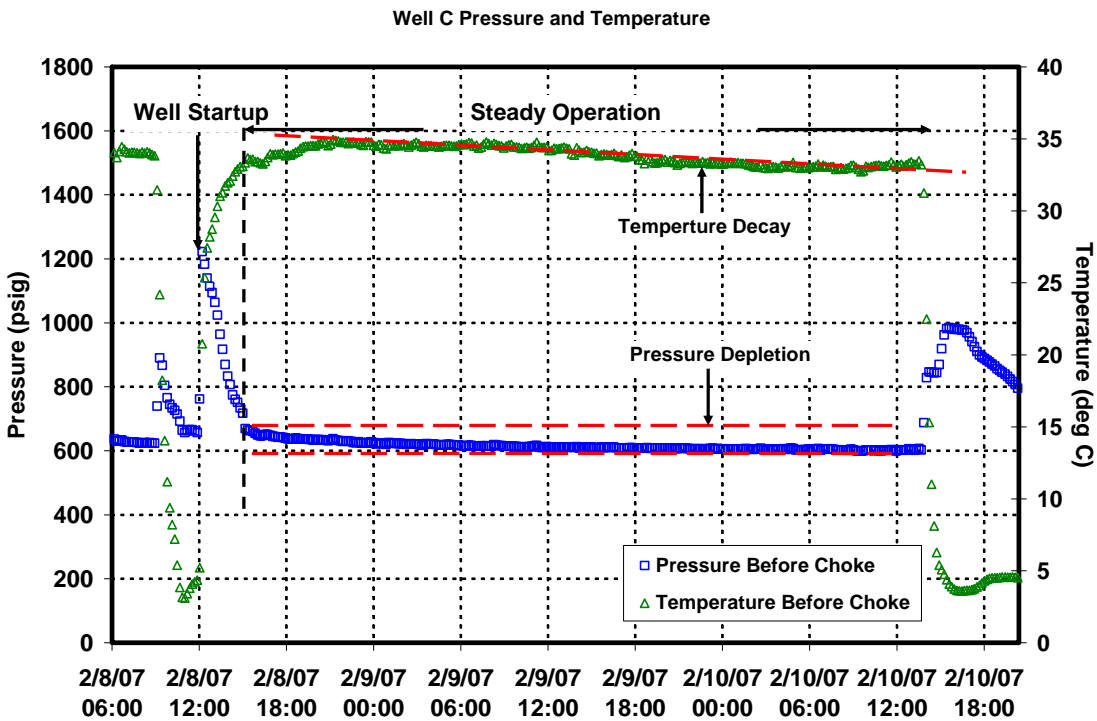


Figure 24: Wellhead pressure and temperature decay after well C startup

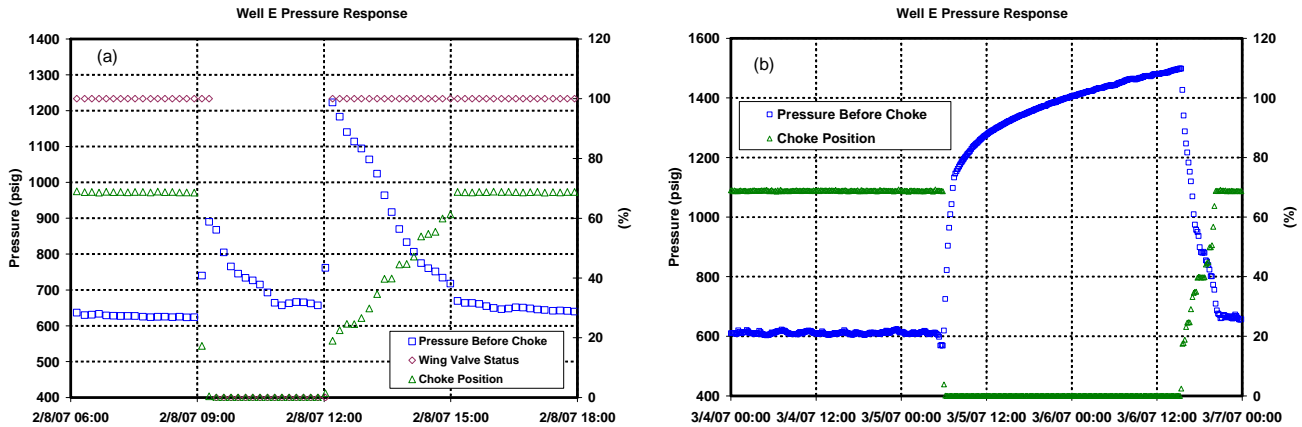


Figure 25: Wellhead pressure response during shut-in when (a) wing valve is closed and (b) when wing valve is left open

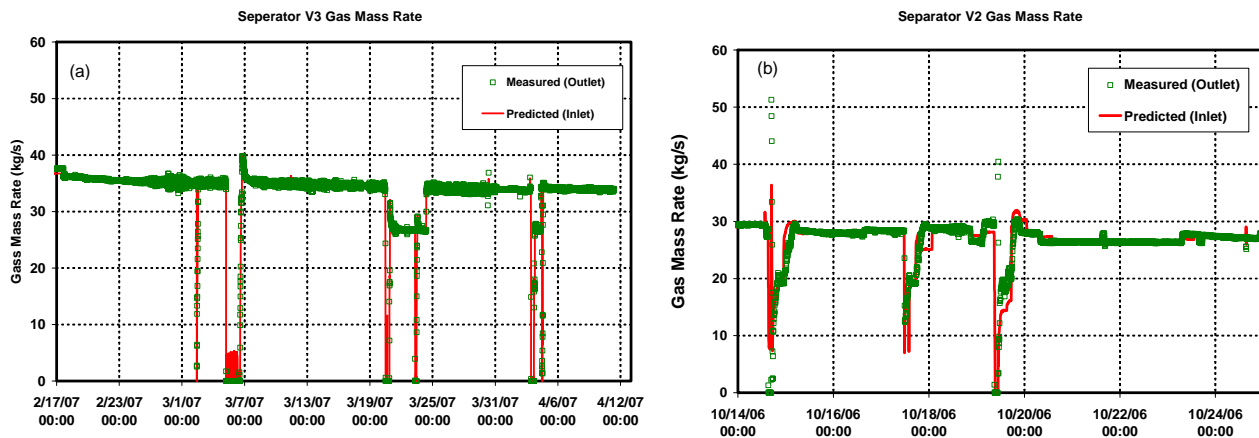


Figure 26: Comparison of predicted vs. measured total gas production at (a) separator V3 and (b) separator V2

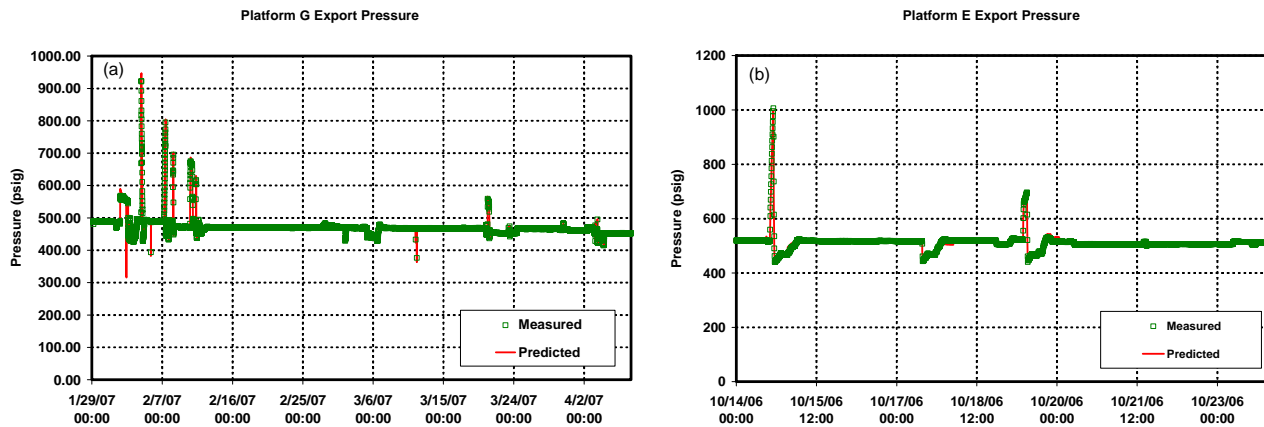


Figure 27: Comparison of measured pressure vs. model predicted pressures for (a) platform G and (b) platform E

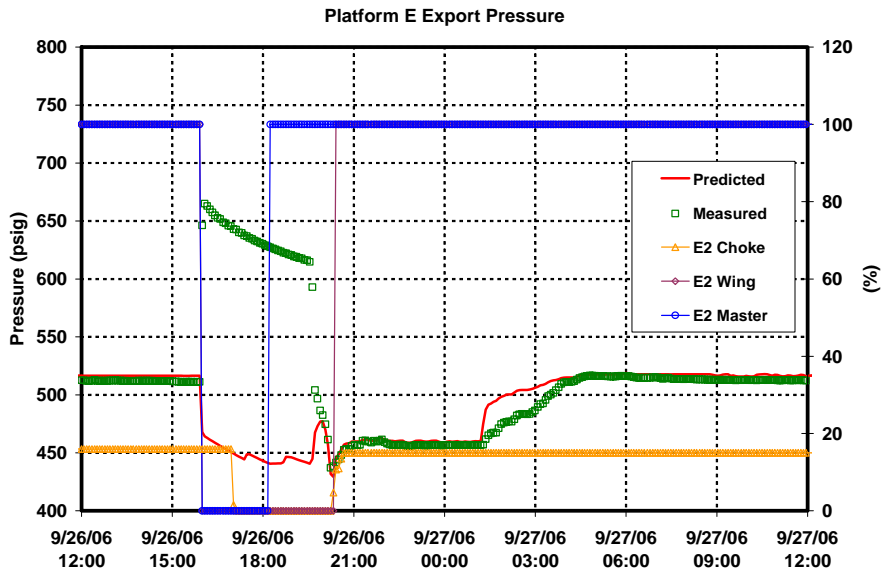


Figure 28: False blockage alarm during emergency shut-down because shutdown valve was not incorporated in model

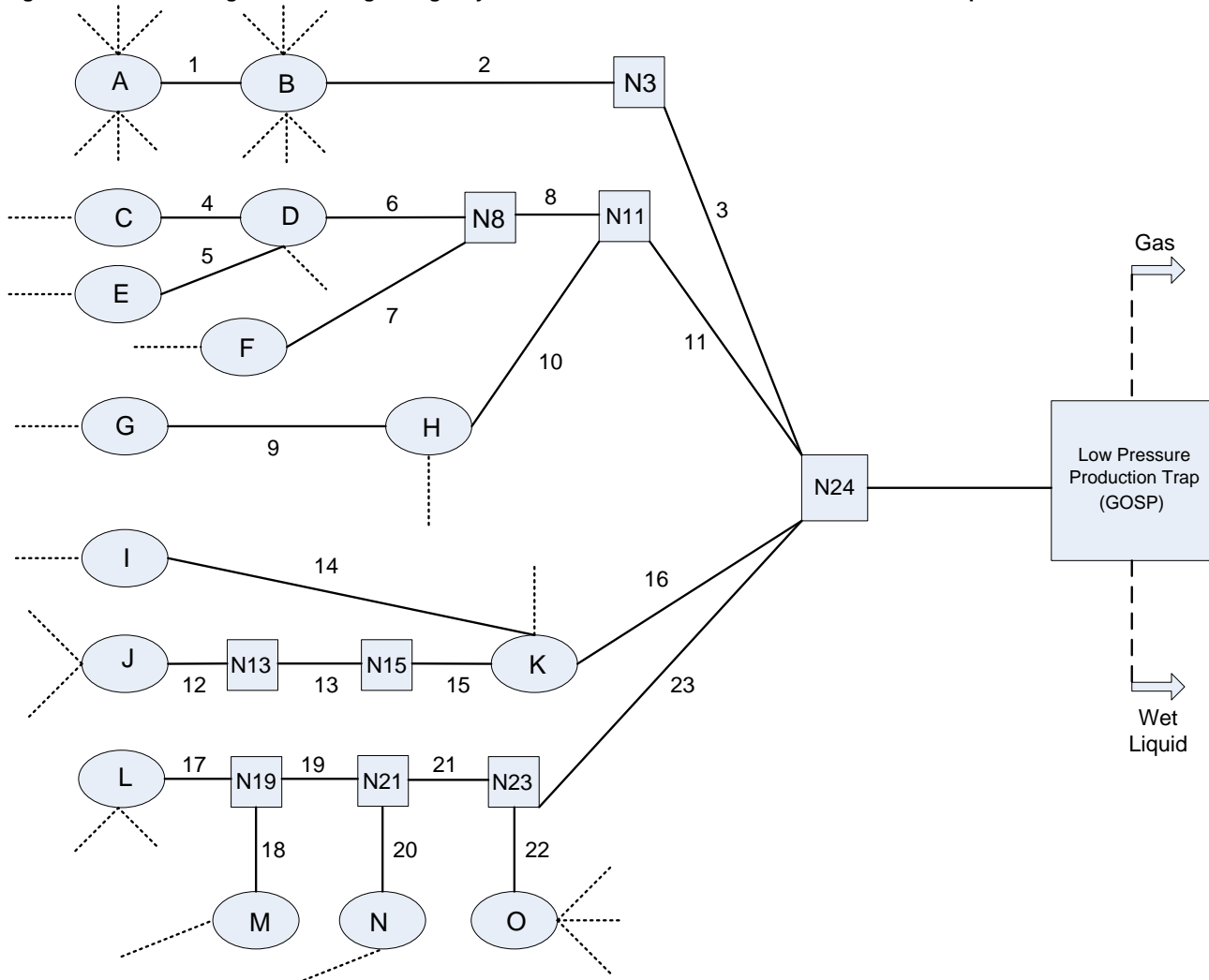


Figure 29: Schematic of pipeline network for medium crude feeding a low pressure separator

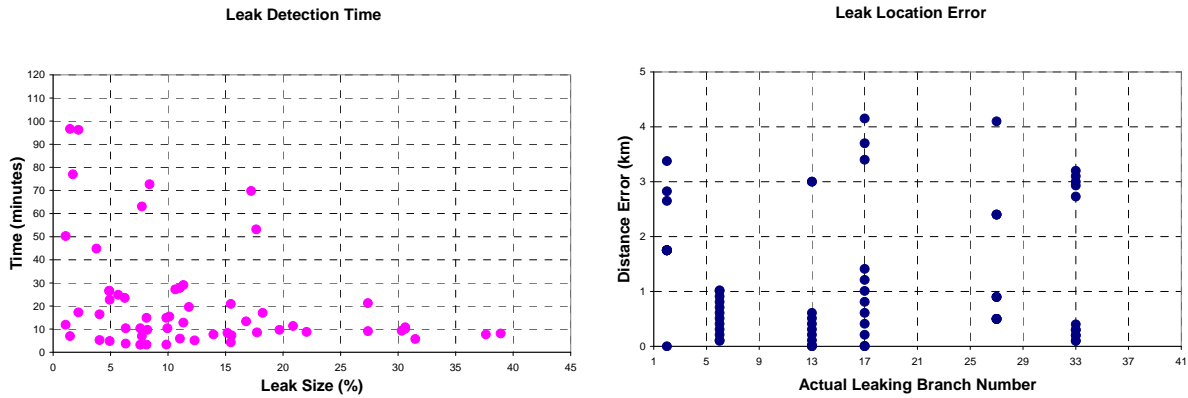


Figure 30: (a) Leak detection time vs. leak size, and (b) leak location errors for different leak points within the network

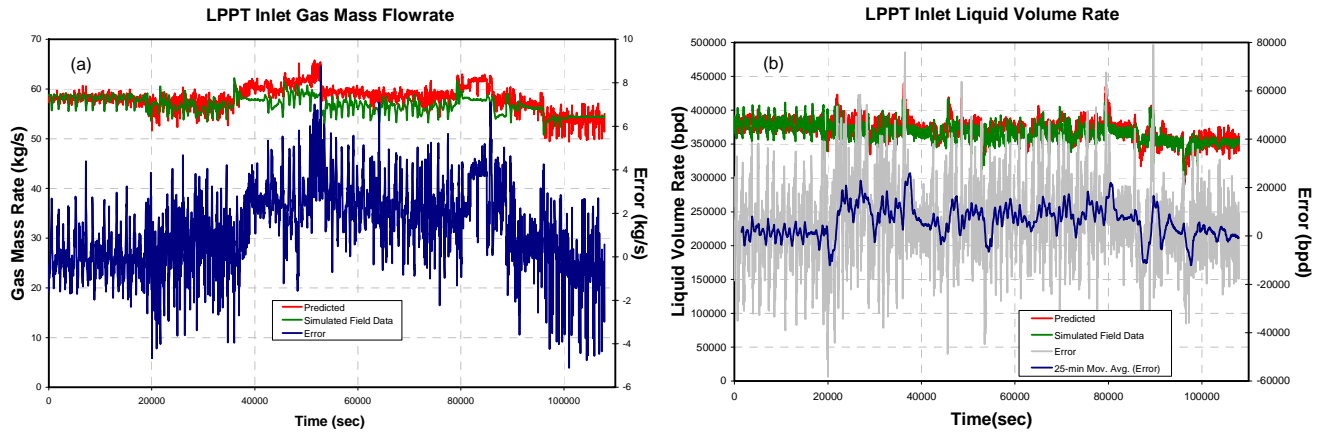


Figure 31: Comparison of model predictions vs. (simulated) field for (a) gas mass rate and (b) liquid volume rate in the event of a 60 mm leak

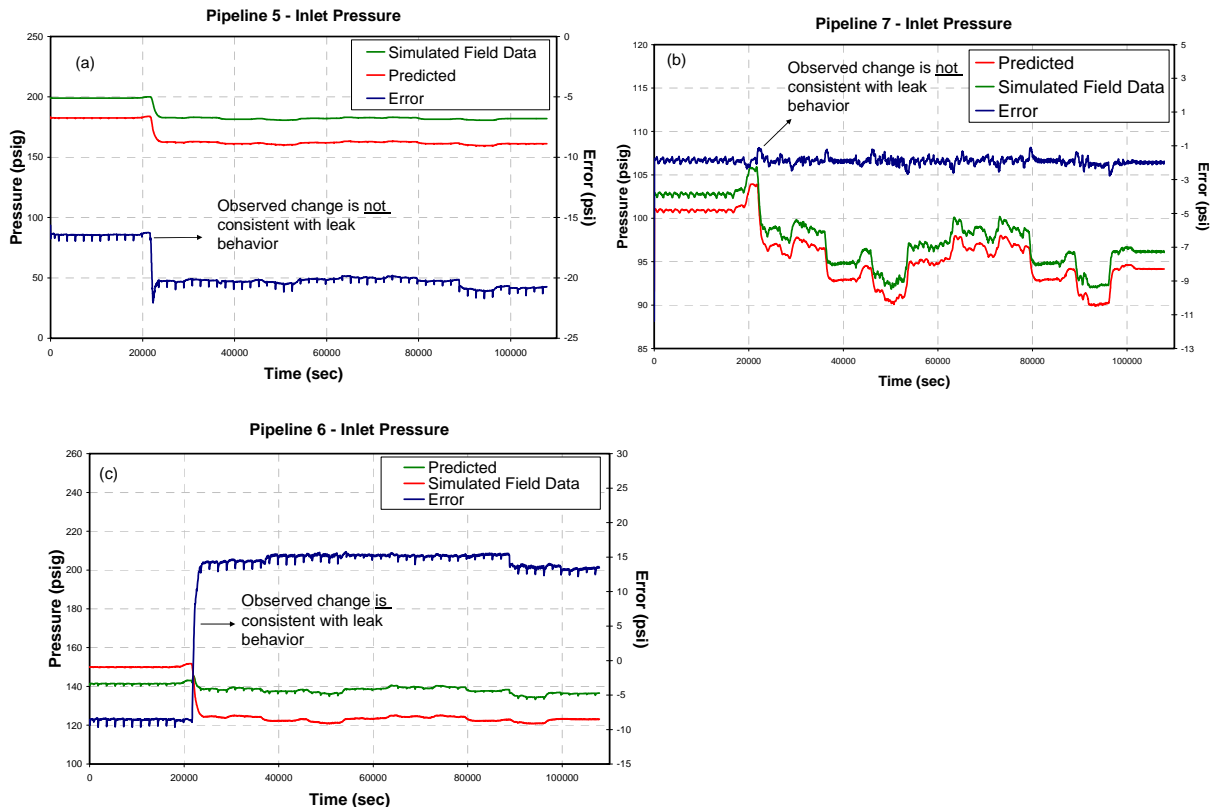


Figure 32: Pressure response within the network in the event of a 60 mm leak in branch 6 and comparison between field pressures and model predicted pressures for (a) branch 5, (b) branch 7, and (c) branch 6